THE DEVELOPMENT AND STUDY OF A RESISTIVITY METHOD OF PROSPECTING APPLICABLE IN VALLEYS; ITS APPLICATION TO THE AZDAVAY CARBONIFEROUS AREA, AND THE CORRELATION OF THE RESULTS WITH THOSE OF SEISMIC, WELL LOGGING AND GEOLOGICAL SURVEYS

Mehmet Y. DİZİOĞLU

Mineral Research and Exploration Institute of Turkey

ABSTRACT.— The need is made clear of the development of a new resistivity method of prospecting applicable in the 2-dimensional valleys. Different methods of attack for the development are discussed. Among these, the method of small-scale model experiments is preferred. The reasons for this preference are explained. An analysis of the errors involved in the experiments is made.

A factor K embodying the effects of the geometrical shape of the valley is introduced and its variation for different types of valley and electrode position is studied. The directional resolving power of the method is investigated.

Then, the method so developed is applied to the Azdavay Carboniferous area with a view of determining the thicknesses and types of different geological formations and of detecting and locating the faults. The results obtained are correlated with the known geology as well as with those of the well logging and seismic surveys conducted in the same area.

INTRODUCTION

There arise many difficulties in applying some of the geophysical methods of prospecting which are developed for the semi-infinite medium, in valleys or in rough terrain. The reasons for these difficulties are as follows :

1. It becomes necessary to conduct the survey in the valley, in a limited space.

2. The discontinuity which produces the anomaly, could be anywhere around the valley. Hence the method and technique used should be able to determine the direction of the discontinuity from the measured anomaly.

3. There are, usually, some materials on the bottom and sides of the valley which affect the geophysical measurements. For instance, there usually exist running water or water accumulations on the bottom. And these are underlain by layers of sand or gravel. Water, on the other hand, reduces the magnitude of the anomaly produced by the discontinuity, due to its low resistivity.

The electromagnetic methods of prospecting may be handicapped by the sides and the conductive layer which usually exists on the floors of the valleys. This effect increases as the conductivity of this layer gets large.

As regards the reflection seismic method of prospecting, it becomes necessary to conduct a separate refraction survey, apart from the main one, in order to

determine the varying thicknesses of the bottom layer and then to apply the weathered layer corrections.

As far as the magnetic methods are concerned, the effects of any abnormally polarized rocks on the sides or bottom, of the valley may prove a disturbing factor.

When using the gravimetric methods it becomes essential to apply carefully the topographic corrections for the sides.

As regards the resistivity methods, in particular, they cannot be applied to valleys in their present state. Because any point in the valley cannot be considered to be in a semi-infinite or infinite medium. On the other hand, the methods so far developed are applicable to these 2 types of medium. Hence, it becomes clear that the development of a new resistivity method of prospecting allowing for the effects of the geometrical shape of the valley is much in need.

Judging from the number of papers published, it can be stated that very little research has so far been done on this subject. The published literature in this line is very scanty and in fact only one important reference was found, viz, «Earth Measurements in the Lake Superior Copper Country» by W. O. Hotchkiss, W. J. Rooney, J. Fisher (A.I.M.E., Geophysical Prospecting, 1929, pp. 51-65).

In this paper the authors describe resistivity measurements made in a stope with an object of checking the thickness of a ledge above the stope. The Wenner method was used and the electrodes were positioned along the gallery. 2 curves were plotted. In one the electrode separations were plotted against the apparent resistivities calculated using the Wenner's formula for surface electrode positions $\varrho = 2\pi a \frac{V}{I}$ (a = electrode separation) and in the other the electrode separations were plotted against the apparent resistivities calculated using Wenner's formula for interior electrode positions $\varrho = 4\pi a \frac{V}{I}$. Since neither of these formulae represented exactly the relation between these resistivities and the observed values, an approximate transition curve was drawn. But very little inference could be obtained from the resulting curve because of the uncertainty as to its position. On the other hand, the part of the curve with large electrode separations could be relied on and was interpreted. This paper is of importance in showing that greater part of the survey was valueless for prospecting purposes, mainly due to the fact that the effect of the stope opening on the relation between the resistivity and the measured current and potential was not known.

Actually, the author of the present thesis has come across the same difficulties in conducting resistivity surveys in different regions of Turkey. In 1951 the development of the method had to be started when the problem of the investigation of the water horizons under a deep valley in the Central Anatolia had to be solved by the author. Later, the same difficulties were encountered in the Azdavay Carboniferous area which is full of deep valleys. The method which had been developed since 1951, both in the laboratories of the M. T. A. Institute and in the field, was used in the Azdavay area and satisfactory results were obtained.

This thesis contains 2 sections :

1. In the first section an account is given of the development and study of a new method of resistivity prospecting applicable in different types of valley. The resolving power of the method is also investigated in this section.

2. In the second section, the method developed is applied in the valleys of the Azdavay Carboniferous area in order to determine the geological structures and to detect and locate faults. The results obtained were compared and correlated with the seismic and well logging surveys made in the same region. And lastly, the results of the 3 surveys were correlated with the known geology and the drill hole sections.

Section I.

THE DEVELOPMENT AND STUDY OF A RESISTIVITY METHOD OF PROSPECTING APPLICABLE IN VALLEYS

I. 1. Method of attack and procedure used.

It is evident that electrodes situated in a valley or in rough terrain cannot be considered as either placed on a plane surface of the conductor or entirely within its volume. Hence, neither of Wenner's (1) resistivity formulae $\varrho = 2\pi a \frac{V}{I}$ or $\varrho = 4\pi a \frac{V}{I}$ applicable in the 2 special cases, represents exactly the relation between the resistivity and the measured current, potential and electrode separation.

It can, however, be proved that the general expression for the resistivity of a homogeneous medium, measured by a 4-electrode system situated in an opening in the medium is $\varrho = K\pi a \frac{V}{I}$, where K is a constant depending on the linear dimensions involved; a is a length and V and I are the potential drop between the potential electrodes and the total current flowing between the current electrodes respectively.

The proof of this theorem is as follows :

In a problem of steady current flow in isotropic and homogeneous media the potential must satisfy Laplace's equation, $\frac{\partial^2 V}{\partial x^2} + \frac{\partial^2 V}{\partial y^2} + \frac{\partial^2 V}{\partial z^2} = 0$ at all points not occupied by a source or sink. At the boundaries the tangential component of the voltage gradient and the normal component of the current flow must be continuous, i. e. $\partial V_1/\partial t = \partial V_2/\partial t$ and $\frac{I}{\varrho_1} \cdot \frac{\partial V_1}{\partial n} = \frac{I}{\varrho_2} \cdot \frac{\partial V_2}{\partial n}$ where V_1 and V_2 are the potentials at each side of the boundary; ϱ_1 and ϱ_2 are the resistivities and $\frac{\partial}{\partial t}$, $\frac{\partial}{\partial n}$ represent differentiation along the tangent and normal to the surface.

In the immediate vicinity of a point source, the potential V at a distance R, is given by $V = \frac{\varrho I}{4\pi R}$

Let / be the measure of the size of the resistivity distribution, i.,e. the linear dimension which specifies the size of some. body. In the model experiments this will be reduced to /' and all other dimensions will also be reduced by the factor I'/l

Then measuring allco-ordinates in terms of / :

$$\xi = \frac{x}{l}, \quad \eta = \frac{y}{l}, \quad \zeta = \frac{z}{l}$$

the above equations reduce to

$$\frac{\partial^2 V}{\partial x^2} + \frac{\partial^2 V}{\partial y^2} + \frac{\partial^2 V}{\partial z^2} = 0 \quad \ldots\ldots\ldots\ldots\ldots\ldots \quad (1)$$

$$\partial V_1/\partial \nu = \partial V_2/\partial \nu$$

$$\frac{I}{\varrho_1} \cdot \frac{\partial V_1}{\partial \nu_2} = \frac{I}{\varrho_2} \cdot \frac{\partial V_2}{\partial \nu_2}$$

$$V = \frac{\varrho I}{4\pi l} \cdot \frac{I}{r} \quad \ldots\ldots\ldots\ldots\ldots\ldots\ldots \quad (2)$$

where $\nu = t/l$, $V = n/l$, and $r = R/l$

Hence, the general expression for the potential must be, from (1)

$$V = f_1 \left(\frac{x}{l}, \frac{y}{l}, \frac{z}{l}\right)$$

Since the potential is directly proportional to the resistivity and the current,

$$V = \varrho \frac{I}{l} \cdot f_2 \left(\frac{x}{l}, \frac{y}{l}, \frac{z}{l}\right)$$

Very near the source, however, the potential must take the form (2) and so finally

$$V = \varrho \frac{I}{4\pi l} \cdot f_3 \left(\frac{x}{l}, \frac{y}{l}, \frac{z}{l}\right) \quad \ldots\ldots\ldots\ldots\ldots\ldots\ldots\ldots\ldots \quad (3)$$

where for small values of x, y, z,

$$f_3 \longrightarrow \frac{1}{r}$$

If the potentials at the potential electrodes are V_1 and V_2 and their co-ordinates are (x_1, y_1, z_1) and (x_2, y_2, z_2) respectively, then

$$V_1 - V_2 = \Delta V = \varrho \frac{I}{4\pi l} \cdot \left\{ f_3 \left(\frac{x_1}{l}, \frac{y_1}{l}, \frac{z_1}{l}\right) - f_3 \left(\frac{x_2}{l}, \frac{y_2}{l}, \frac{z_2}{l}\right) \right\}$$

multiplying the right-hand side by $\frac{\alpha}{a}$ and arranging,

$$\varrho = \pi \alpha \frac{\Delta V}{I} \cdot K$$

where

$$K = \frac{4\,l}{a} \cdot \frac{I}{f_3\left(\frac{x_1}{l}, \frac{y_1}{l}, \frac{z_1}{l}\right) - f_3\left(\frac{x_2}{l}, \frac{y_2}{l}, \frac{z_2}{l}\right)}$$

thus proving the theorem stated above.

The formula (3) also justifies the use of a scale model for resistivity measurements. Since the same potential distribution on a small scale is retained, if, in the model, the value of $\varrho\, I / l$ is maintained equal to its value on the large field scale.

In the simple case of a half a cylindrical valley in a uniform semi-infinite medium, with the line of the electrodes along the top edge of the valley, then with the Wenner system of 4 equally spaced contacts, the potential difference V between the inner electrodes is,

$$V = \frac{2\,\varrho\, I}{4\,\pi\, l}\left\{f_3\left(\frac{a}{l}, 0, 0\right) - f_3\left(\frac{2\,a}{l}, 0, 0\right)\right\}$$ where a = electrode separation

or

$$V = \frac{\varrho\, I}{\pi\, a} \cdot \frac{a}{2\,l}\left\{f_3\left(\frac{a}{l}, 0, 0\right) - f_3\left(\frac{2\,a}{l}, 0, 0\right)\right\}$$

if the origin of the co-ordinate axes occupies the position of the first current electrode and the x-axis is along the top edge. Since for a given electrode separation $\frac{a}{l}$ is the same in field and in model

$$\varrho = \pi\, a\, \frac{V}{l} \cdot K$$

where

$$K = 1 \Big/ \frac{a}{2\,l}\left\{f_3\left(\frac{a}{l}, 0, 0\right) - f_3\left(\frac{2\,a}{l}, 0, 0\right)\right\}$$

If the medium is not homogeneous then this expression will give the apparent resistivity.

In order to develop and study a resistivity method applicable in 2 - dimensional valleys, small-scale model experiments were made using different types of valley. For each type of valley, the values of the factor K were determined with different positions of the line of electrodes. The resistivity formulae so determined were studied for different types of geological structures which occur frequently in the nature.

These experimental studies were made with a view to forming a set of fundamental data to aid the interpretation of the future resistivity surveys in valleys.

It should be noted that the development of the method could also be obtained by mathematical analysis — at least in theory — and such results would be free from experimental errors. The reasons for the preference of small-scale tank experiments were that the solutions of 3-dimensional potential problems are very lengthy and difficult and involve expressions frequently cumbersome to be of practical value for numerical calculations. On the other hand, the technique for the small-scale model experiments is simple and rapid in operation.

As will be seen later, such experiments, involve some disturbing factors, but they can be assessed where necessary.

For these reasons, the development of the method by the small-scale experiments is preferred to that by the rigid mathematical calculations.

I. 2. Apparatus and equipment employed for the small-scale model experiments.

The layout of the apparatus for the small-scale model experiments is shown in Fig. 1.

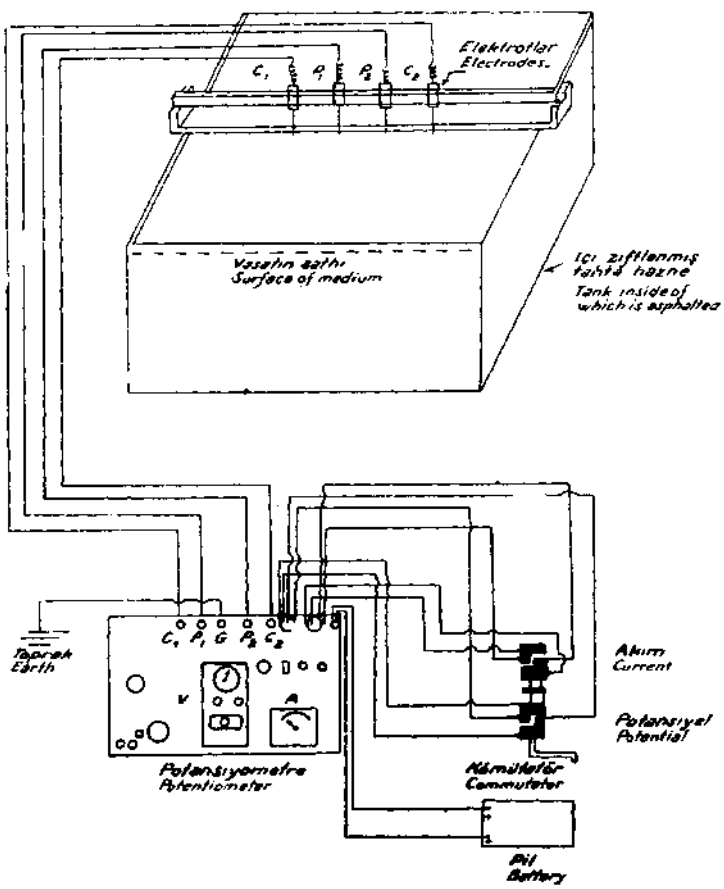

Fig. 1 - Layout of the apparatus and equipment used in the model experiments

To produce the semi-infinite medium, a tank was made of wood and coated with pitch to prevent leakage of the salt solution inside it. The models were positioned in this medium at the required position, and using the Wenner-Gish-Rooney system, resistivity measurements were made on the models. The apparatus employed for these measurements are manufactured by the Geophysical Instrument Co., U.S.A.

The electrodes, about 12 cm long, were made of aluminium or silver. To secure a point source or sink, the ends of the current electrodes were pointed,

and to make good contact with the equipotential lines on the surface of the tank-water, the ends of the potential electrodes were chisel-edged. In the experiments, these edges were positioned parallel to the neighbouring equipotential lines. This procedure reduced the error with which the potential differences could be measured.

The electrodes with their sliding holders were mounted on a rack which could, as a whole, slide backward and forward across the tank. The electrodes were insulated from the metallic slides by means of ebonite rings.

The circuit diagram of the geophysical potentiometer is shown in Fig. 2. This potentiometer can measure potential differences up to 1.12 volts with an accuracy of 0.5 mV. It also incorporates a selector switch to select any of the potential differences between the terminals P_1, G, P_2. The instrument works on the null principle. The null point is indicated by an optical galvanometer.

A condenser of 20 microfarads could be connected in series in the potential circuit. The reason for this is to eliminate the parasitic potentials of outside source as well as the antisymmetrical position effects when the Wenner-Gish - Rooney system of measurements is used.

The potentiometer is designed to work in conjunction with a commutator as well as to measure D.C. potentials.

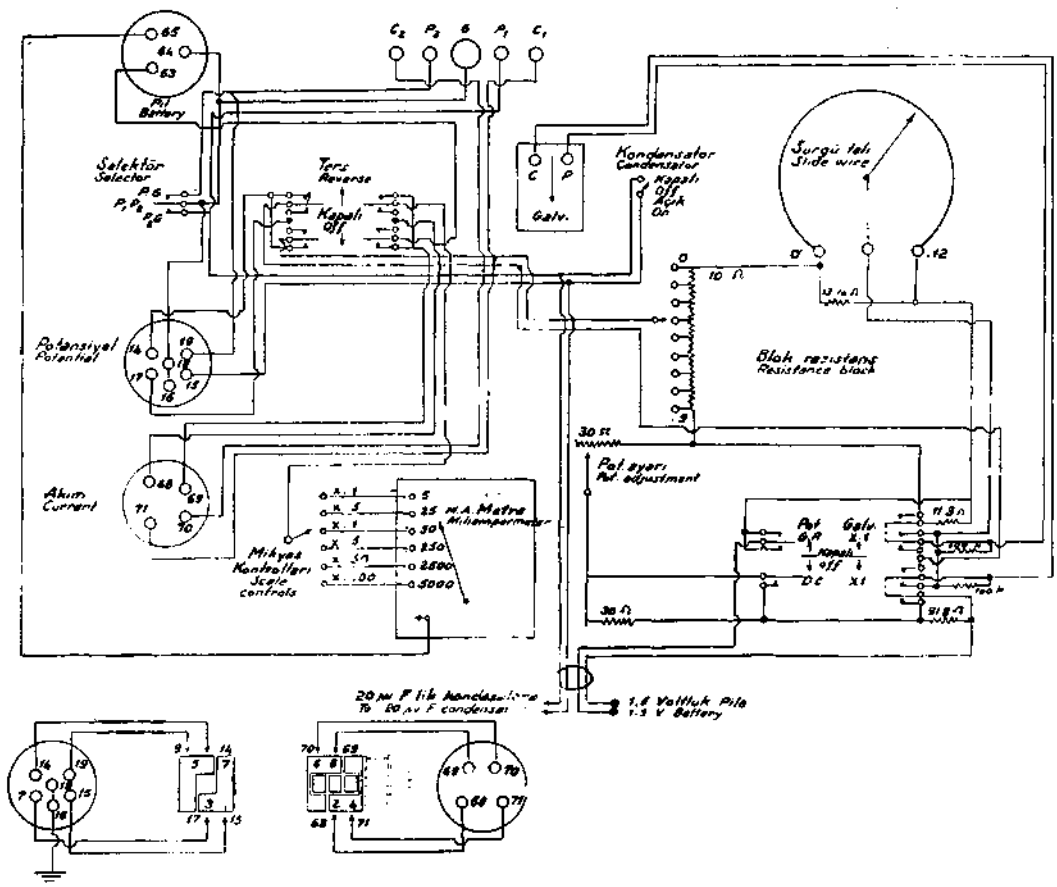

Fig. 2 - Circuit - diagram of the geophysical potentiometer for the deep Gish - Rooney resistivity method

The potentiometer box incorporates also a D. C. milliampermeter which measures the current used in the resistivity measurements (Fig. 2) This multi-range milliampermeter has 50 divisions on it. Each division corresponds to 0.1, 0.5, 1, 5, 50, 100 mA for different positions of the range switch. So it covers from 5 mV to 5A for full-scale defection.

To eliminate the effects of polarization potentials, a hand-driven double commutator (20-30 revs./sec.) was inserted in the measuring circuit, as shown in Fig. 1.

I. 21. Design of a small-scale tank and determination of its dimensions.

Resistivity measurements made at the surface of a medium in a model tank, using a 4-electrode system will be affected by the walls and the base of the tank due to their disturbing effect on the distribution of the current.

This effect will increase as the current electrodes approach the walls. Hence, in deciding the size and shape of the tank, the material for the construction, the type of electrode configuration, the maximum spread of the electrodes to be used must be considered in relation to the required accuracy of the measurements.

For the model experiments in this thesis, Wenner's configuration of electrodes was used and it was decided that 12 cm separations would be the maximum necessary.

With these two requirements in mind, some trial calculations were made in order to determine the magnitudes of the effects of the tank walls on the measured tank-water resistivity. For these calculations it was assumed that the tank was rectangular in shape, made of insulating material and that the centre of the electrode system was in the middle of the tank with the line of electrodes parallel to one side.

No formula exists which permits the precise calculation of the effects of the walls and the base of the tank, and therefore an approximate calculation was made. The effects were divided into three parts :

1. The influence of the finite thickness of the surrounding medium, i. e. the effect of the base of the tank.
2. The influence of the walls parallel to the line of electrodes.
3. The influence of the walls perpendicular to the line of electrodes.

1. An approximation to the effect of the base of the tank was calculated using the two-layer resistivity formula (2)

$$\varrho a = \varrho_1 \left[1 + 4 \sum_{n=1}^{\infty} \left\{ \frac{k^n}{\left[1 + 4n^2\left(\frac{h}{a}\right)^2\right]^{1/2}} - \frac{k^n}{\left[4 + 4n^2\left(\frac{h}{a}\right)^2\right]^{1/2}} \right\} \right]$$

or

$$\varrho a = \varrho_1 \left\{ 1 + F_1 (a, h) \right\}$$

Where ϱa is the apparent resistivity measured with Wenner's configuration of electrodes, at the electrode separation (a), for two layers, the resistivity of the

lower one (base of the tank) being infinity, while the depth and the resistivity of the upper one (medium in the tank) being *(h)* and (J_1) respectively. In this formula *K* represents the ratio $\frac{\varrho_2 - \varrho_1}{\varrho_2 + \varrho_1}$

Strictly speaking, this formula applies if the medium in the tank was of infinite lateral extent but to an approximation J1. *F1 (a, h)* was taken as the total anomaly due to the base of the tank only.

2. The same formula gives the apparent resistivity for the case where a medium of resistivity *(*J_1) is situated between two parallel non-conducting planes of semi-infinite extent, the line of electrodes being on the surface of the medium and mid-way between.

This theorem can be proved easily using the image methods.

Hence, to an approximation J_1. F_1 *(a, l)* (where / is the distance of the line of electrodes from one of the walls) could be taken as the total anomaly due to the two sides of the tank which are parallel to the line of electrodes.

3. The effect of one of the walls perpendicular to the line of electrodes can be calculated, assuming that the wall and the medium were of semi-infinite extent. For this purpose, using the method of images, the following apparent resistivity formula can be derived,

$$\varrho\, a = \varrho_1 \left[1 + \cdot \frac{4\,b}{a_r} \left\{ \frac{1}{4\left(\frac{b}{a}\right)^2 - 4} - \frac{1}{4\left(\frac{b}{a}\right)^2 - 1} \right\} \right]$$

or

$$\varrho\, a = \varrho_1 \cdot (1 + F_2) \quad \ldots\ldots\ldots\ldots \quad (1)$$

where J *a* is the apparent resistivity measured using Wenner's configuration of electrodes positioned in a semi-infinite medium of resistivity J1 with the line of electrodes perpendicular to the insulating boundary wall; the electrode separation and the distance of the centre of the electrode system from the wall being *a* and *b* respectively.

2 F_2 . J_1 could be taken, to an approximation, as the total anomaly due to the two sides of the tank which are perpendicular to the line of electrodes. An idea of the magnitude of the error in the apparent resistivity, arising from this approximation can be obtained from a consideration of the effects of the infinite number of secondary images due to the two walls.

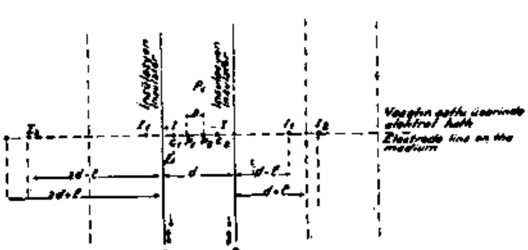

Fig 3 - Distribution of the images

From Fig. 3 it will be seen that the positions of the images with respect to the walls are as follows:

Distance of I_1 on the left side of the wall (A) from the wall (A) l

» I_2 » » $2d - l$

» I_3 » » $2d + l$

» I_4 » » $4d - l$

» I_5 » » $4d + l$

» In (n is even) » $nd - l$

or

» In (n is odd) » $(n-1)d + l$

Distance of I_1 on the right side of the wall (B) from the wall (B) ..... $d - l$

» I_2 » » $d + l$

» I_3 » » $3d - l$

» I_4 » » $3d + l$

» I_5 » » $5d - l$

» I_6 » » $5d + l$

» In (n is even) » $(n-1)\,d + l$

or

» In (n is odd) » $nd - l$

The potential difference Vn between P_1 and P_2 due to a pair of images (In) s, with n being even, is :

$$Vn = \frac{\varrho_1 I}{2\pi}\left\{\frac{1}{(nd-l)+l+a} - \frac{1}{(nd-l)+l+2a} + \frac{1}{(n-1)d+l+l+2a} - \frac{1}{(n-1)d+2l+a}\right\}$$

making use of the relation

$$l = \frac{1}{2}(d - 3a)$$

$$Vn = -\frac{\varrho_1 I}{2\pi} \cdot \frac{1}{(n^2 d^2 - a^2)\,(n^2 d^2 - 4a^2)}$$

The potential difference Vn' between P_1 and P_2 due to a pair of images (In) s, with n being odd, is :

$$Vn' = \frac{\varrho_1 I}{2\pi}\left\{\frac{1}{(n-1)d+l+l+a} - \frac{1}{(n-1)d+l+l+2a} + \frac{1}{nd-l+l+2a} - \frac{1}{nd-l+l+a}\right\}$$

$$Vn' = \frac{\varrho_1 I}{2\pi} \cdot \frac{6\,n\,d\,a^2}{(n^2 d^2 - a^2)\,(n^2 d^2 - 4a^2)}$$

Hence, the total potential difference Vt between P_1 and P_2 due to the images of the source I and the source I itself,

$$Vt = (-1)^{n+1} \cdot \frac{\varrho_1 I}{2\pi} \cdot \sum_{n=1}^{\infty} \frac{6\,n\,d\,a^2}{(n^2 d^2 - a^2)\,(n^2 d^2 - 4a^2)} + \frac{\varrho^1 I}{2\pi} \cdot \frac{1}{2a}$$

The total potential difference V between P_1 and P_2 due to the source I and the sink $-I$ is $2\,Vt$

Hence, the apparent resistivity $\varrho\,a \left(= 2\pi a \ \frac{V}{I}\right)$ is

$$\varrho_a = \varrho_1 \left\{ 1 + 2\,(-1)^{n+1} \sum_{n=1}^{\infty} \frac{6\,n\,d\,a^3}{(n^2 d^2 - a^2)\,(n^2 d^2 - 4\,a^2)} \right\}$$

and

$$F'_2 = (-1)^{n+1} \cdot \sum_{n=1}^{\infty} \frac{6\,n\,d\,a^3}{(n^2 d^2 - a^2)\,(n^2 d^2 - 4\,a^2)}$$

Now, a numerical comparison of $2\,F_2'$ with $2\,F_2$ [see Formula (1)] will enable us to estimate the error arising from the approximation.

For the biggest electrode separation (a = 12 cm) used and with a width of 100 cm between the walls (d = 100 cm) :

$2\,F_2$ = 2 X 0.01120.

On the other hand,

$2\ F_2'$ = 2 (0.01120 — 0.001205 + 0.000384 — 0.000162 + 0.00083 —....)

It will be seen that the terms in the series for $2\,F_2'$ decrease in magnitude very quickly; in fact with big ratios of $\frac{d}{a}$,

$$F_2' = (-1)^{n+1} \cdot \frac{6a^3}{d^3} \cdot \sum_{n=1}^{\infty} \frac{1}{n_3}$$

from a comparison of the above numerical values for $2F_2$ and $2\,F_2'$, it can be seen that the error in $2F_2$, i. e. the error due to the approximation, is smaller than

$$\frac{0.001}{0.0112} = 9\ \%$$

For the same width between the walls the error due to the approximation will be smaller as the electrode separation decreases due to the increase in the ratio $\frac{d}{a}$.

The approximate total fractional variation from the actual resistivity J_1 of the tank-water is $F1\ (a,h) + 2F_2 + F_1\ (a,\ l)$. The results for different tank dimensions and electrode separations are shown in the Table I. It can be seen

TABLE I

a Electrode separation in cm	$F_1\ (a,\ h)$ h=depth of tank h=30cm	h=35 cm	$2\ F_2$ $b=\frac{90}{2}$ cm	$b=\frac{100}{2}$ cm	$F_1\ (a,\ l)$ $l=\frac{80}{2}$ cm	$l=\frac{90}{2}$ cm	$l=\frac{100}{2}$ cm	$F_1\ (a,h) + 2\ F_2 + F_1\ (a,l)$ total fractional variation for sizes ($=h \times 2b \times 2l$ cm^3) 35×90×90	35×100×90	35×100×100
4		0.0012		0.00039×2		0.00			0.0020	
6		0.0040		0.0013 ×2		0.0018			0.0084	
8		0.0088		0.00317×2		0.005			0.0200	
10	0.029	0.0200	0.009×2	0.0063 ×2	0.012	5.0092	0.0064	0.047	0.0418	0.039
12		0.0318		0.0112 ×2		0.015			0.069	

that the effect due to the base of the tank is the biggest and the effect due to the sides perpendicular to the line of electrodes is bigger than that due to the other sides for the same electrode separations when $b = l$.

The dimensions chosen were,

depth = 35 cm ; side parallel to the line of electrodes 100 cm
» perpendicular » » » 90 cm

for the following reasons :

1) For determinations of the factor K_s, it was decided to use electrode separations not greater than 8 cm and at this separation the variation from the true resistivity, with the chosen dimensions of the tank, is about 2 percent, which was considered to be good enough for the purpose.

2) Electrode separations up to 11-12 cm were to be used for other experiments. Although these separations correspond to high-percent variations (about 6%), the relative values and variations rather than the absolute values of apparent resistivities were important in these experiments and the anomalies measured with 11-12 cm separations would in general be much larger than the necessary corrections for the wall effects.

3) A bigger size of tank would be inconvenient for use by a single person, since the electrodes and the middle of the tank would not be easily accessible.

To determine the actual percentage corrections to the resistivity of the tank-water, 2 trials were run with the tank filled with solutions of different salt concentrations.

The experimental percentages, together with those calculated, are plotted against the electrode separation in Fig. 4. It will be seen that the theoretical curve follows closely the experimental results. The mean percentages were calculated from the experimental curves and used to correct for the finite size of the tank for all other small - scale tank experiments. The actual resistivity of the tank-water was determined, in each case, with 3-4 cm separations for which the correction is negligible.

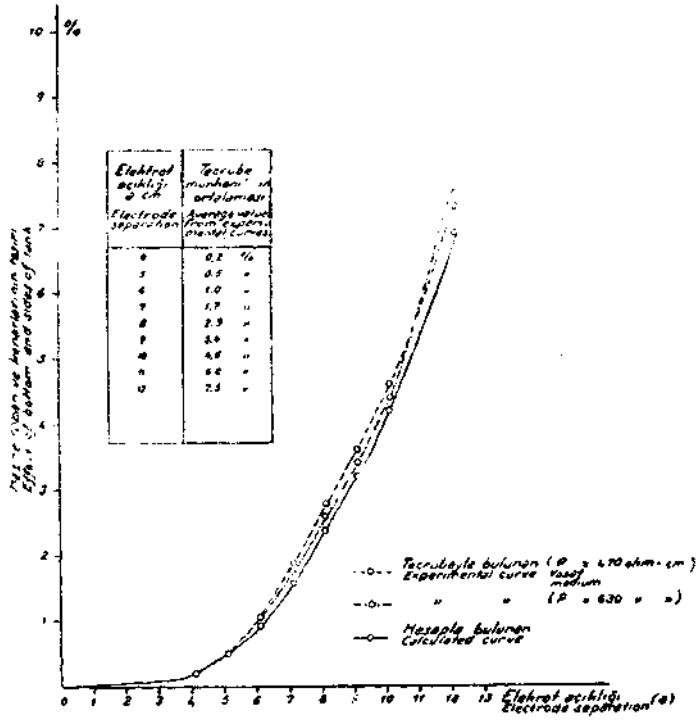

Fig. 4 - Correction curves for the sides and bottom of the tank

I. 3. Method of determining the Factor K.

It has already been explained that if Wenner's electrode configuration were used and the electrodes were placed along a valley situated in a homogeneous medium of semi-infinite extent, the resistivity of the medium would have the form

$$\rho = K \pi a \frac{V}{I} = K \pi a R$$

where the symbols a, *V*and *I* have the significances already defined, and *R* is the observed resistance between the potential contacts. Thus K=J/a.*R*. Therefore to determine the factor *K* for a valley by small-scale experiments, the model valley made of an insulating material is to be immersed in the homogeneous medium of the tank-water, so that top edges coincide with the surface of the medium and with electrodes along the valley, then measurements of *V,I* and *a* are taken and *K* is then calculated from the above formula. Since the tank was of limited dimensions it was necessary to make the best use of its size.

In selecting the electrode separations most suitable for the determination of the factor *Ks,* two factors had to be considered :

1) The error in the measured values of *V* and *a* will increase as the electrode separation gets smaller. The error in *V* will be due to,

a. the fact that the equipotential lines get closer as the electrode separation decreases,

b. the increase in the irregular volume of the tank-water in contact with the model tunnel.

The error in (a) will mostly arise from the finite thickness of the electrodes.

2) With larger electrode separations the effect of the tank walls on V gets larger.

For these reasons a compromise was necessary. An electrode separation between 5-8 cm was found to be most suitable since at these separations F could be measured with adequate accuracy and the variation from the actual resistivity of the tank-water was less than 2 percent.

The experimental procedure adopted in the determination of the factor *K* was as follows :

1) The depth of the tank-water with the model valley in, as indicated above, was adjusted to a pre-fixed value for which the percentage variations from the actual resistivity of the tank-water were known.

2) With the model removed, the resistivity of the tank-water was measured with a separation of 4 cm.

3) The model was then replaced with the electrodes along its side already described and five readings of *V* and *I* were then taken for each electrode separation. For each reading the positions of the electrodes and the model were read-

justed. The mean value of $\left(\frac{V}{I}\right)_s$ was used in the formula

$$K = \frac{\varrho\,(1 + r_a\,\%)}{\pi\, a \dfrac{V}{I}}$$

where is the actual resistivity of the tank-water; r_a is the percentage variation from the resistivity of the tank-water at the electrode separations (Fig. 4).

It should be added here that it was much easier to position the electrodes along the top edges of the model valleys than along the other edges. For the latter positions, the electrodes were nailed through the valley into the medium. When the electrodes for one separation were used, they were then sealed off by an insulating material to prevent their contacts with the medium.

To show the magnitude of errors involved in the model experiments as well as the general procedure, some measurements for the determination of the factor K for a valley of half a cylindrical shape, with the electrodes along its top edge, are given below in Table II.

TABLE II

a = electrode separation; d = diameter of the half a cylindrical valley.

$\frac{a}{d}$	a cm	d cm	$\frac{V}{I}$ mV/mA	Mean $\frac{V}{I}$	$\varrho_a = \varrho\,(1 + ra\,\%)$ where $\varrho = 240$ ohm - cm	$K = \varrho_a / \pi a \frac{V}{I}$
2	6	3	8.15 8.16 8.20 8.21 8.15	8.17	2.42	1.575
4	8	2	5.40 5.43 5.45 5.46 5.40	5.43	245.50	1 83
10	7.5	0.75	5.45 5.47 5.50 5.49 5.46	5.475	245	1.90

I. 4. Analysis of the errors involved in the factor K.

To eliminate roughly the errors in the factor *Ks,* due to the finite size of the tank, the apparent resistivity J_e of the tank - water which included the effect of the walls, was used in the calculations :

$$K = \varrho_e \,/\, \pi a \frac{V}{I}$$

This can be readily justified :

In an infinite tank $K = \varrho / \pi a \frac{V'}{I}$ ..... **(1)**

where V is the potential difference which would be observed with the electrode separation a in a medium of resistivity J. The effect of the walls modifies both the resistivity to J_e and the observed potential to V, according to the equations :

$$\varrho_e = \varrho \ (1 + r_a \%)$$
$$V = V' \ (1 + r_a \%)$$

substituting the values of J and V from these into (1), the working equation becomes:

$$K = \frac{\varrho_e}{1 + r_a \%} \Big/ \frac{\pi a V}{I(1 + r_a \%)}$$

or

$$K = \varrho_a \Big/ \pi a \frac{V}{I}$$

The other errors which may arise are due to the experimental errors in the measurement of $V\backslash I$ and of a, the finite thicknesses of the electrodes, the positions of the contacts relative to the cylinder and, finally, the setting of the cylinder with a diameter on the surface.

An idea of the error in K, due to the error in the measurement of V/I, can be obtained by finding the probable error in the arithmetical mean of the measured values of V/I and then the corresponding probable error in the factor K, assuming the other quantities have no errors. The probable error of the arithmetical mean is given by

$$r_0 = 0.6745 \sqrt{\frac{\Sigma v^2}{n(n-1)}}$$

where v is the residual and n is the number of observations.

As seen from the values of $V\backslash I$ in the above Table II, the residuals are roughly the same and equal to about 0.02, whence

$$r_0 = 0.6745 \sqrt{\frac{.02^2 \times 5}{4 \times 5}} = 0.0067$$

The corresponding probable error in the factor

$$K = \frac{\varrho \ (1 + r_a \%)}{\pi a \ \frac{V}{I}}$$

is $\pm \frac{\partial K}{\partial \left(\frac{V}{I}\right)} \times r_0 = \pm \frac{\varrho \ (1 + r_a \%)}{\pi a \left(\frac{V}{I}\right)^2} \times r_0$

and the percentage probable error is

$$\pm \frac{r_0}{\frac{V}{I}} \times 100 = \pm \frac{0.67}{\frac{V}{I}}$$

In the measurements, the values of $\frac{V}{I}$ varied from about 5 up to 18. The percentage probable errors in the factor Ks, corresponding to these values are 0.13 and 0.037 respectively, the average being about 0.1.

The error due to the finite thicknesses of the electrodes and the positions of the contacts can be estimated approximately as follows :

Let us take the worst possible case, supposing that the true positions of the potential contacts are P_1 and P_2 and their wrong positions are P_1' and P_2' while C_1 and C_2 being the true positions of the current electrode contacts (see Fig. 5).

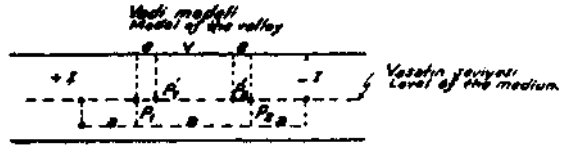

Fig. 5

The potential difference V between P_1' and P_2' is approximately :

$$V = 2\frac{\varrho I}{K\pi}\left(\frac{1}{a+e} - \frac{1}{2a-e}\right)$$

where ϱ is the resistivity of the medium and e is the distance $P_1 P_1' = P_2 P_2'$

$$V = \frac{2\varrho I}{K\pi}\cdot\frac{(2a-e)-(a+e)}{(a+e)\ (2a-e)}$$

$$V = \frac{2\varrho I}{K\pi}\cdot\frac{(a-2e)\ (1-e/a)\ (1+e/2a}{2a.a}$$

or

$$V = \frac{\varrho I}{K\pi a}\cdot(1-2e/a)\ (1-e/a)\ (1+e/2a)$$

which is approximately equal to :

$$V = \frac{\varrho I}{K\pi a}\left(1 - \frac{4e}{2a} - \frac{2e}{2a} + \frac{e}{2a}\right)$$

$$V = \frac{\varrho I}{K\pi a}\left(1 - \frac{5e}{2a}\right)$$

Whence the percentage error in V is $\frac{5e}{2a} \times 100$.

The corresponding error in the factor K is about the same. It will be seen that the error increases as the electrode separation decreases. Assuming that the displacement e is about $\frac{1}{8}$ mm, the percentage errors in the factor Ks for the biggest and smallest electrode separations (4 and 9 Cm) are 0.78, 0.35 respectively, the average being about 0.6.

Finally, the errors due to the setting up of the cylinder and the measurement of the electrode separation would be negligibly small, since linear measurements can be measured as accurately as required.

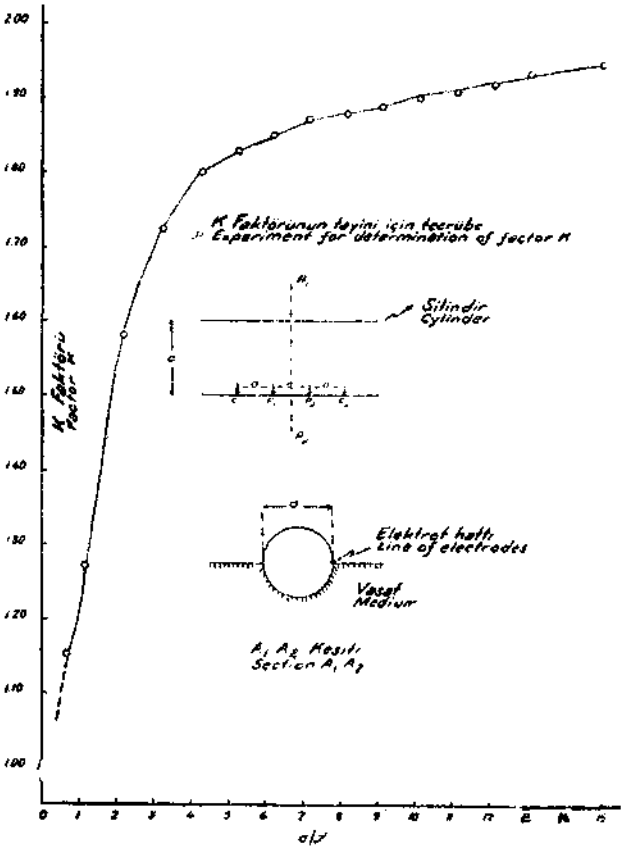

Fig. 6 - Variation of the factor K with a/d for a valley having a semi - circular cross - section

In conclusion, it appears that the total errors in the determined values of the factor *Ks* are less than 1 %.

It should be mentioned here, that the commutator factor does not introduce any error in the determination of the factor K, since it appears at both the numerator and the denominator of the expression for the factor *K*, cancelling itself out.

The results are plotted in Fig. 6. It is seen that the rate of variations of the factor *K* with *a/d* is very large up to *a/d = 5*, after which it slows down. Therefore in choosing the values of the factor *K* for up to *a/d=5*, much care must be taken.

If the factor *K* for a/d =8 is taken as 2, instead of the actual value, then the error made would be about 6 %.

I. 5. Determination of the factor K for different positions of the line of electrodes positioned in different types of valley and study of its variation with the type of valley and electrode position.

The factor was determined with the accuracy shown above, for different types of 2- dimensional valleys, the line of electrodes being at different positions.

As regards the resistivity surveys, the valleys occurring commonly in nature could be divided into 4 main types :

1) The type with a cross-section of right-angle triangle, the right angle being at the bottom corner. This type of valley occurs frequently in the crystalline and intrusive area.
2) The type with a half a circle cross-section. The ondulations in the alluvium-covered plains are usually of this type.
3) The type with a rectangular cross-section, the height of which being half the base.
4) The type with a square cross-section. Deep river or stream beds form this type.

The other types of valley could be treated as the interpolation of these 4 main types. Hence, the values of the factor *K* were determined for these types. The dimension specifying the valley was taken to be its top width *(d).*

I 51. Variation of the factor K with the 4 types of valley when the electrodes are positioned along the top edge of the valley.

The variation of the factor K with the ratio of a/d for each type of valley is shown in Fig. 7. It will be seen from this figure that the effect of the valley on the measurements is negligibly small when the electrode separation is about 15 times the width of the valley.

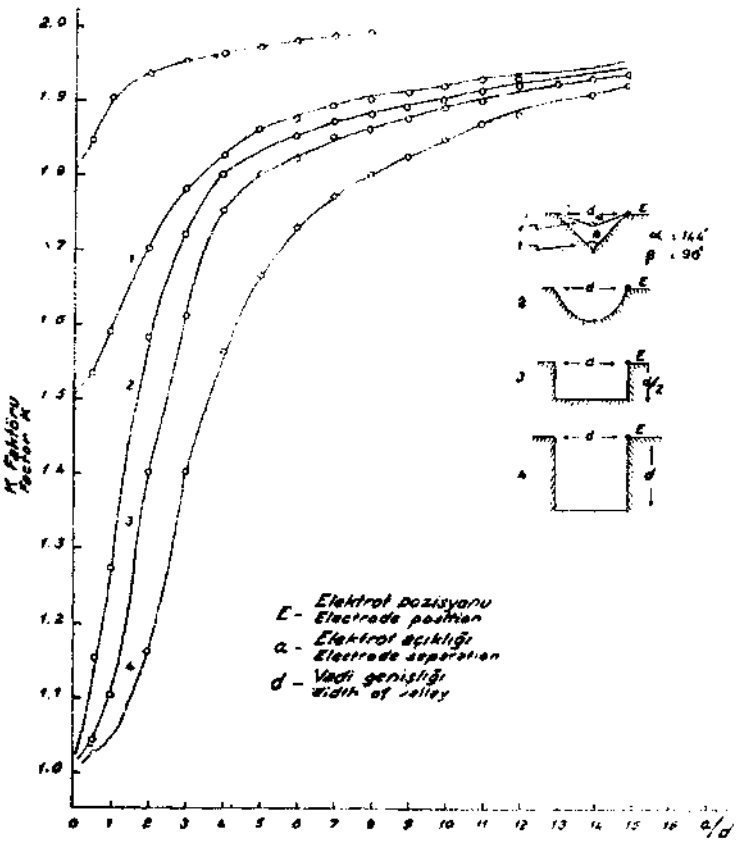

Fig. 7 - Variation of the factor K for different types of valley. (Electrodes positioned along the top corners)

Each curve exhibits 2 points of maximum curvature, and an inflection point between. For instance, the inflection point for the 4th type of valley occurs when $a/d = 3$, and the maximum curvatures occur when $a/d = 1.5$ and 5. For the other types, these points change place slightly.

It is evident from these considerations that it is necessary to be careful when evaluating the values of the factor K between the two maximum curvatures, especially around the inflection point.

From the curves it will be seen that when the value of the ratio of a/d approaches zero, the value of the factor approaches :

1.5	for	the	1st	type
1	»	»	2nd	»
1	»	»	3rd	»
1	»	»	4th	»

These limiting values can be checked rigidly using the potential theory or the method of images.

As regards the magnitudes of the values of the factor, for the same values of a/d $(a/d > 1)$, the values of K for the 4th type are 15 % smaller than those of the 2nd. Those of the 1st type are the greatest and those of the 3rd lie between those of the 2nd and 4th.

I. 52. Variation of the factor K with the 4 types of valley when the electrodes are positioned along the bottom or bottom corner of the valley.

These variations are shown in Fig. 8. Again, the effect of the body of the valley becomes negligibly small when the electrode separation is around 15 times the width of the valley. When the value of the ratio of *a/d* approaches zero, the values of the factor approach 3, for the 1st, 3rd, and 4th types of valley and it approaches the value of 2 for the 2nd type.

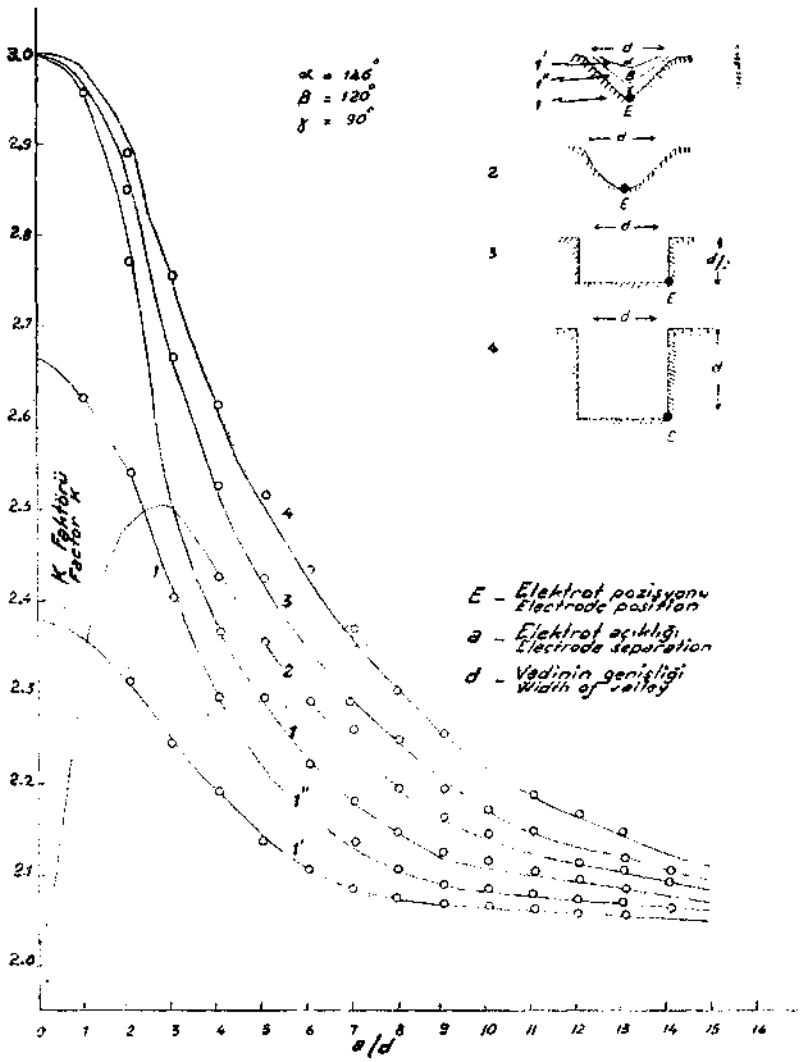

Fig. 8 - Variation of the factor K for different types of valley (Electrodes positioned along the bottom corners)

For the 1st, 3rd and 4th types, each curve exhibits 2 points of maximum curvature and an inflection point in between,. The second maximum curvature points occur when *a/d* is about equal to 6. For this reason, it is to be careful in choosing the values of the factor which lie between the values of zero and 6 of

the ratio *a/d,* for the 1st, 3rd and 4th types of valley. The curve for the 2nd type shows one maximum curvature and 2 inflection points.

For the practical purposes, the rate of variation of the factor K with *a/d* can be considered to be large up to *a/d* = 7.

I. 53. Variation of the factor K with the 4 types of valley when the electrodes are positioned along the middle of the bottom or side of the valley.

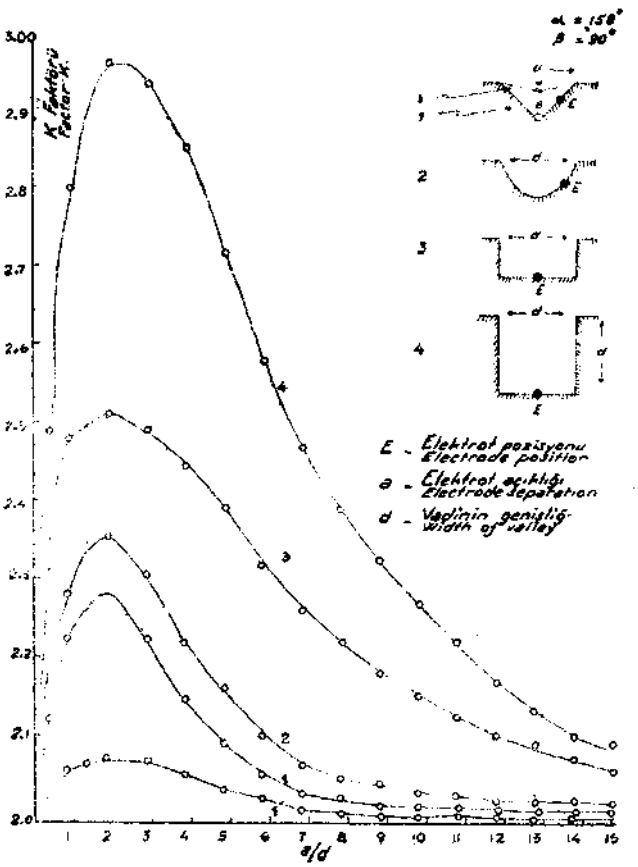

Fig. 9 - Variation of the factor K for different types of valley (Electrodes positioned along the middle of the bottoms or sides)

The positions of the electrodes and the curves obtained are shown in Fig. 9. The effect of the body of the valley gets negligibly small when the value of *a/d* approaches 15 for the 3rd and 4th types and 7 for the 1st and 2nd types.

When *a/d* approaches zero, the value of the factor decreases down to 2 for all/the types.

Each curve exhibits one maximum point around *a/d* = 2. For the same values of *a/d,* the values of the factor *K* are greater for the 4th type than for the 3rd and smaller for the 2nd type than for the 3rd The smallest values occur for the 1st type. Because as the body of the valley involved in the measurements gets smaller as compared with the electrode separation, the value of the factor approaches 2.

The large rate of variation of the factor corresponds to the values of *a/d* between 0-2 and 2-6 for the 3rd and 4th types and to the values of *a/d* between 0-2 and 2-5 for the 1st and 2nd types.

I. 6. Study of the potential distribution around the valley and the investigation of the resolving power of the method.

By means of these studies, it was intended to estimate the usefulness and the limitations of the method under ideal conditions and to obtain a set of basic data to aid interpretations of actual field surveys.

I. 61. Distribution of the potential around a valley of the form of a half-cylinder.

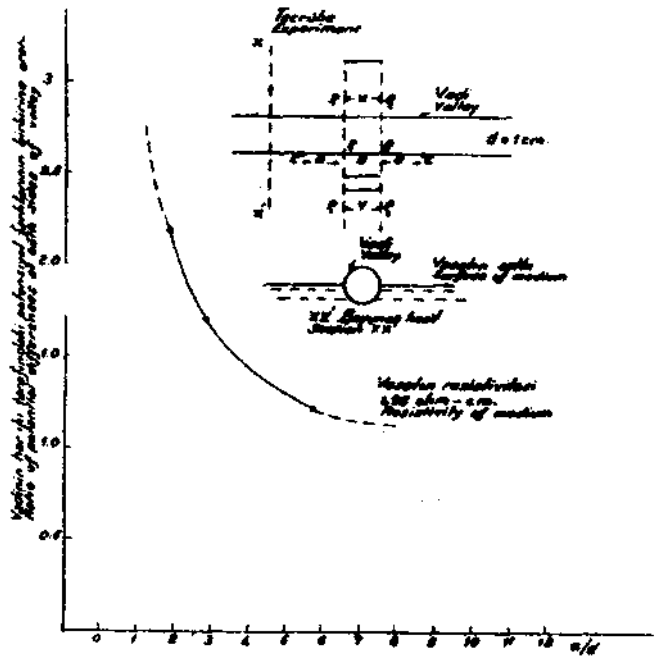

Fig. 10 - Variation of potential around a valley

To investigate this distribution, the electrodes were positioned along the edge of a model valley as shown in Fig. 10, and then the potential electrodes at a fixed separation were moved along a direction at right angle to the axis of the model. By this procedure the average ratios of potentials (V_1/V_2) on both sides of the model valley and at the same distance from the line of current electrodes were measured and plotted against electrode separation (Fig. 10). It will be seen that the rate of change of the ratio with electrode separation is very large up to the value of $a/d = 3$ and small beyond $a/d = 6$; in the interval between these, it is transitional.

The high concentration of the. current on one side of the valley for $a/d < 2$, indicates that if the body is near enough to give an anomaly, then the difference between the apparent resistivities measured with the electrodes at the near and far sides of the cylinder will be readily detectable. Thus the direction of the body will be indicated.

I. 62. Study of the resolving power of the method.

To study the resolving power of the method, a non-conducting medium represented by a stretched rubber sheet was placed parallel to the axis of the model valley and perpendicular to the surface of the tank-water. The sheet extended to the base and to the two sides of the tank. Then resistivity measurements were made with the electrodes lined along the two top edges of the valley. The experimental arrangement and curves are shown in Figs, 11 and 12.

In order to see the different characteristics of the curves, experiments were made for different distances of the plane from the model valley. Apparent resistivities were also computed for the same positions of the electrodes in the absence of the valley and these were plotted with the corresponding experimental curves in order to ascertain the correspondence between them.

Before beginning to discuss and stud the resistivity curves, it would be useful to state the following theorem :

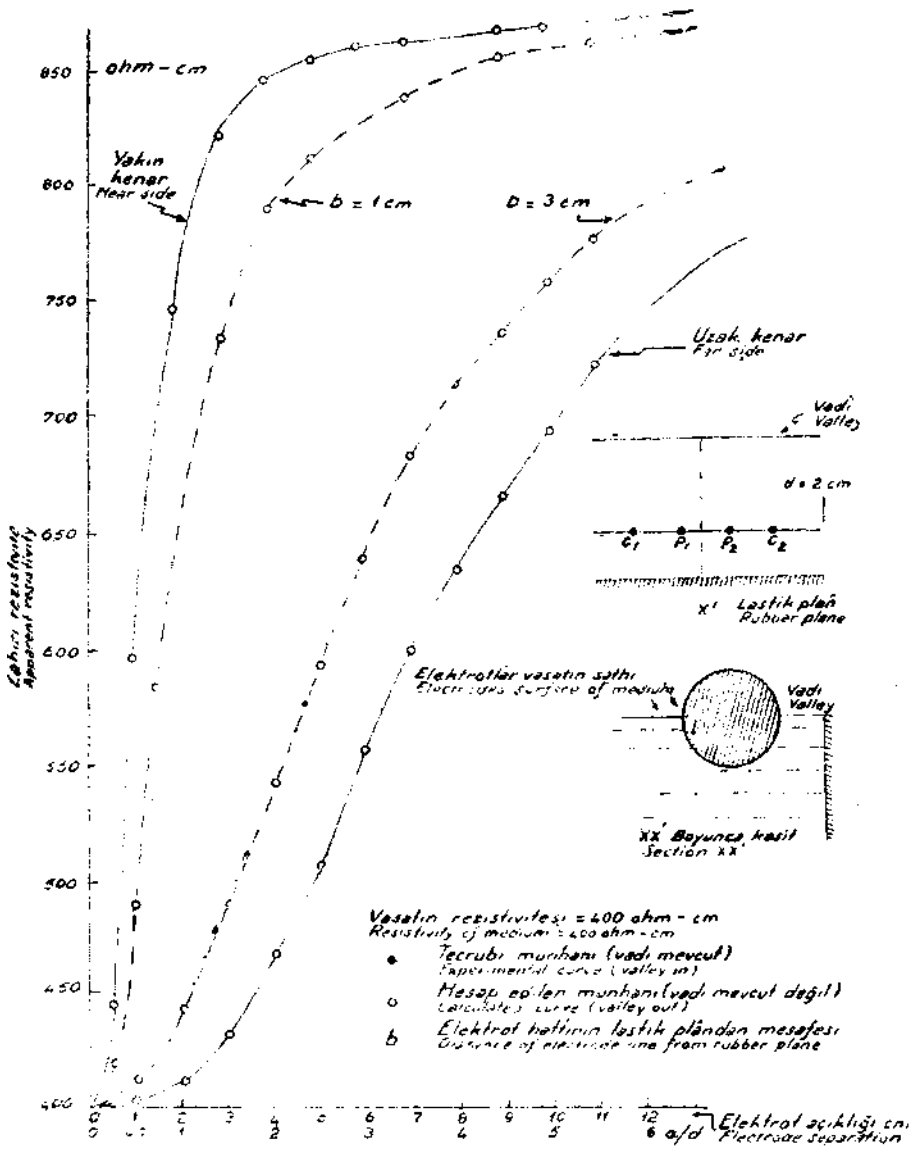

Fig. 11 - Investigation of the directional resolving power of the method

It can be shown that the apparent resistivity 0.9 due to a non-conducting medium with a plane surface of infinite dimensions, measured with Wenner's electrode configuration and with the line of electrodes parallel to the plane interface, is given by

$$\varrho_\beta = \varrho_1 (1 + F_1) \quad \ldots\ldots (1)$$

where $F_1 = k \left\{ \frac{2}{(4\lambda^2 + 1)^{1/2}} - \frac{1}{(\lambda^2 + 1)^{1/2}} \right\}$

and

ϱ_1 = actual resistivity of tank-water

$\lambda = \frac{b}{a}$

a = electrode separation

b = distance of line of electrodes from the sheet

$k = \frac{\varrho_2 - \varrho_1}{\varrho_2 + \varrho_1} = 1$, since in the present case the resistivity of the second layer is infinite.

A consideration of the curves in Figs. 11 and 12 will permit the following conclusions to be drawn :

1) The experimental curves lie outside the corresponding computed curves.

This can be confirmed by considering the apparent resistivity due to a medium of resistivity J_1 between 2 non-conducting media, the electrodes being on one of the interface [see Formula (2) below] and the effect on the apparent

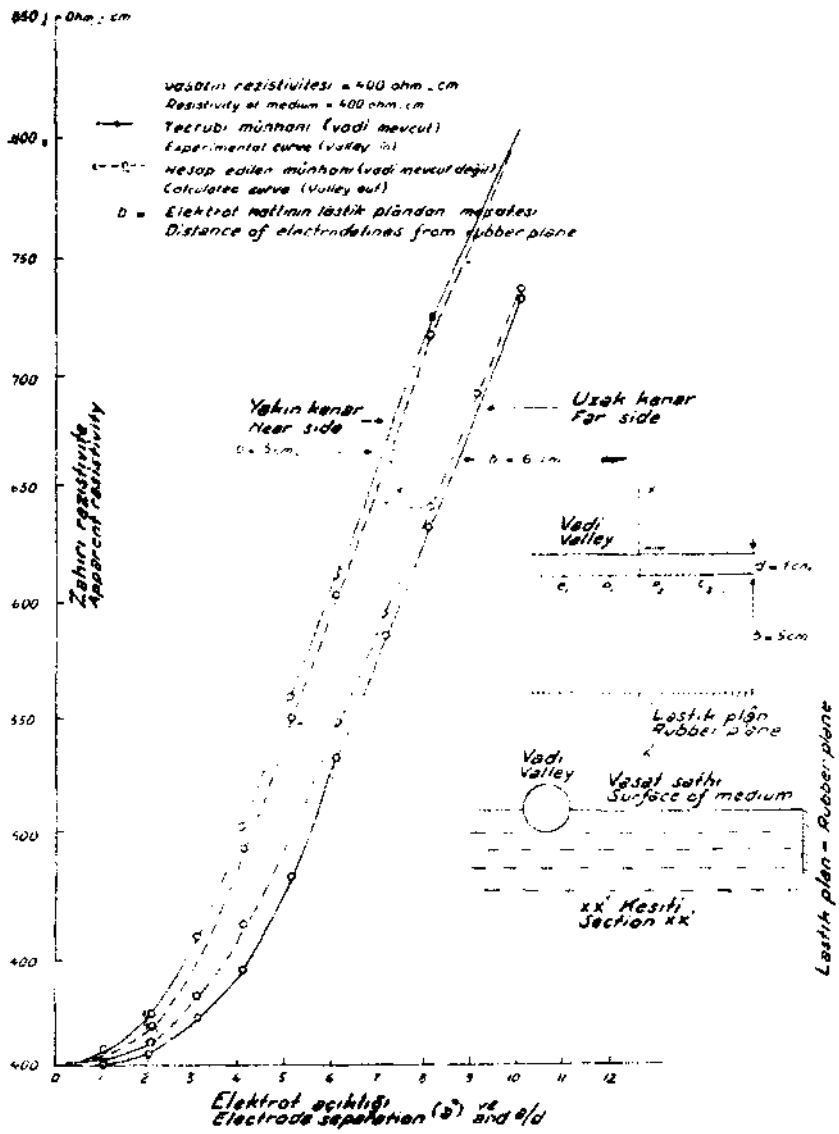

Fig. 12 - Investigation of the directional resolving power of the method

resistivity, of removing the interface passing through the electrodes to infinity without changing the initial position of the electrodes.

$$\varrho_a = \varrho_1 (1 + F_2) \quad \ldots\ldots (2)$$

where $F_2 = 2 \sum_{n=1}^{\infty} k^n \left\{ \frac{2}{(1 + 4n^2\lambda^2)^{1/2}} - \frac{1}{(1 + n^2\lambda^2)^{1/2}} \right\}$

ϱ_a = apparent resistivity for 2 layers of resistivity ϱ_1 and ϱ_2, electrodes being on the surface of the first layer (ϱ_1).

$\lambda = \frac{b}{a}$

b = thickness of first layer

a = electrode separation

$k = \frac{\varrho_2 - \varrho_1}{\varrho_2 + \varrho_1}$ (if $\varrho_2 = \infty$ $k = 1$)

It can be seen that for the same values of λ and ϱ_1, ϱ_a is bigger than ϱ_β.

Now, when the electrode separation is small enough to make the factor K equal to about 2, the current will distribute itself entirely on the side of the electrodes and very little current will go on to the other side of the valley. Hence, Formula (2) will give a close approximation to the conditions and the resistivity anomaly will be bigger with the electrodes at the near side than the corresponding anomaly with the valley out.

As to the far side, with very small separations very little current will pass on to the other side of the source and sink; this being due to the shielding effect of the valley as explained earlier. Hence, the apparent resistivity with the valley in will be smaller than the corresponding one with the valley out. Theoretically speaking, the corresponding curves will meet when the electrode separation becomes infinitely large.

A comparison of the Formulae (1) and (2) will show that

$$F_2 = 2 F_1 \quad \text{if } \lambda > 5$$

and

$$F_2 < 2 F_1 \quad \text{if } \lambda < 5$$

which indicate that for the same electrode separation, the percentage deviation of the experimental apparent resistivity from the calculated one will increase as the distance of the line of electrodes from the interface gets smaller. This deduction can be verified by considering the experimental and the calculated curves in Figs. 11 and 12.

2) The first turning point where the curvature is biggest occurs when the electrode separation is equal to about half the distance between the sheet and the line of electrodes for both the experimental and computed curves.

3) The electrode separation at which the biggest difference between the measured anomalies occurs is the same for the corresponding pairs of experimental and theoretical curves.

For the theoretical curves this separation can be calculated and is given by

$$a = 2\left[\frac{b_1^2 \cdot b_2^{4/3} - b_2^2 \cdot b_1^{4/3}}{b_1^{4/3} - b_2^{4/3}}\right]^{1/2}$$

where b_1 and b_2 are the distances of the line of electrodes from the second medium.

4) For $\frac{a}{b} > 7$ the computed curves (valley out) nearly coincide with the experimental ones (valley in).

Section II.

APPLICATION OF THE RESISTIVITY METHOD DEVELOPED TO THE AZDAVAY CARBONIFEROUS AREA AND THE CORRELATION OF THE RESULTS OBTAINED WITH THOSE OF SEISMIC, WELL LOGGING AND GEOLOGICAL SURVEYS MADE IN THE SAME AREA

INTRODUCTION

The Azdavay Carboniferous area is located 80 km northwest of Kastamonu. Between Azdavay and Kastamonu, there is the Ballıdağ mountain chain which rises 800 m above the level of Azdavay. The distance of the nearest port, Gide, is about 80 km from Azdavay. The road between them has many steep slopes and sharp turnings. The most striking features of the Azdavay area, which is full of valleys, are landslides and creeps. Outcrops of solid rock are quite rare. Even in steep valleys, irregularities in strikes and dips point out to the occurrences of landslides; The best outcrops are, however, found in these valleys. Trenches, 3 meters deep, do not reach the solid seams in many localities between the valleys. They only reveal the disturbed coal seams.

The geological surveys in the Azdavay area, which exhibits a complicated tectonics, could not provide the required information due to the fact that the region is covered by landslides and alluvium. Even some of the geological data obtained could only be interpreted with uncertainty. For these reasons it was decided to use the geophysical methods to solve the problems which had not been cleared by the geology. The combination of the seismic, resistivity and well logging methods were employed in an attempt to solve the problems such as the correlation of different geological blocks and unities, the elucidation of the tectonical structure of the Carboniferous and of the other formations, the determination of the thicknesses and the types of various formations, the detection and location of faults and formation boundaries.

The Azdavay area was first visited and examined in April 1954 from the point of view of the possible application of the geophysical methods and the surveys were started. The seismic, resistivity and well logging surveys were finished at the end of November 1954.

I. 1. Geology of the Azdavay Carboniferous Area. (3)

As it will be seen from Fig. 13,. the dimensions of the Azdavay inlier are 6 km in N-S direction and about 1 km in E-W direction. The western limit is

a great fault which has thrown the Carboniferous about 2000 m down. The eastern limit of the inlier is a Permian cover in the north and a fault in the southern half. The continuation of the Carboniferous under the Permian at a reachable depth in view of mining can be estimated to be 2 km.

Fig. 13 (1/5,000) shows the geological map with the geological formations, faults, trenches with sample numbers (sometimes with topographical survey numbers) and the most likely outcrops of the coal seams. Also the proposed incline with drifts and 3 proposed drilling locations with the estimated depth are shown.

I. 11. Stratigraphy.

1) *Cretaceous.*

The Cretaceous formation in this region consists of limestone, marl and flysch. It covers the western and eastern part of the inlier.

2) *Permian.*

In this formation no fossils are found. The Permian consists of hard sandstones and conglomerates, mosily red in colour, sometimes green. It is covered by the Cretaceous flysch, which also contains no fossils. The basis of the Permian is sometimes a conglomerate, but mostly a sandstone. The dip of the Permian is 40-55°, not parallel to the plane of transgression upon the Carboniferous.

3) *Carboniferous.*

The Carboniferous is exposed on a horst with Cretaceous to the west and Permian to the east. It shows a strike which is almost parallel to the length of the inlier and a dip of about 40° in the eastern direction.

It was found that the youngest formation occurs near Giraç köy, close to the west of fault 1; the age of this formation is Westphalian D-E. The oldest formation, on the other hand, is determined to be Westphalian C.

The age of a sample taken between the seams A and B is found to be Westphalian Upper C. The seams D and Y-E are, on the other hand, Westphalian B-C-D and C-D respectively.

I. 12. Geological Structures.

The Cretaceous and the Permian form a monocline which is slightly folded in a flat syncline and a flat anticline. The strike is N 10-30° E. The almost N-S fault No. 4 caused the downthrow of the westernly block to such an extent that the Carboniferous of the inlier is now in contact with the Cretaceous flysch. The Carboniferous to the west of the fault No. 4 is unattainable for mining, because flysch covers Malmurgon limestones which have a thickness of 600 m.

The Carboniferous forms a syncline with a faulted core (fault 1) and most likely an anticline under the Permian. The greater part of the Carboniferous inlier is a monocline which dips towards east. This part is slightly ondulated and forms the western part of the syncline. This western part of the syncline is also faulted by the faults No. 2 and 3. The block between these faults forms a horst, formed by W.C. mostly, whereas the parts to the west and east are formed by W.D.

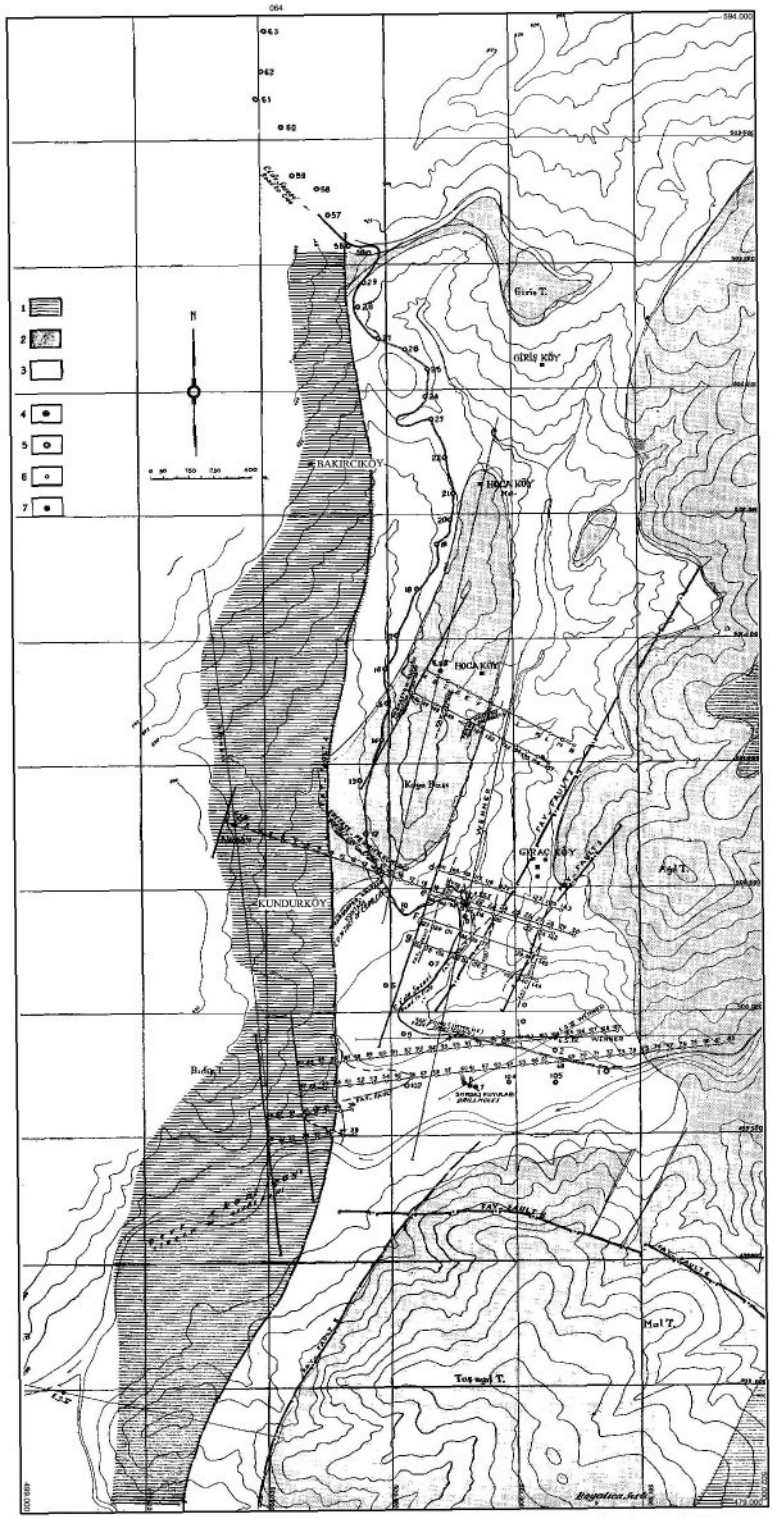

Fig. 13 - Geological Map of the Azdavay Carboniferous inlier with geophysical and drill hole locations (M. Dizioglv)

1- Cretacaous; 2 - Permian; 3 - Carboniferous; 4 - Locations of drillholes; 5 - Locations of seismic shot holes
6 - Resistivity stations; 7 - Locations of resistivity soundings

The folding of the Carboniferous and the faulting by the faults 1, 2 and 3 were pre-Permian. Only the fault No. 1 has a small post-Permian movement, resulting in an uplift of 50 m of the eastern block.

In the southern part of the area, the monoclinal Cretaceous of the east lies upon the Permian with a conspicuous unconformity.

The Permian itself forms an anticline with an axis of about N 20° W, which might be dipping slightly to the north. The monoclinal Permian of Azdavay-North forms the continuation of the eastern limb of this anticline. Fault No. 5 with a downthrow of the eastern part forms the western limit of the Permian. The Carboniferous is exposed on the horst between the faults No. 4 and 5.

I. 2. Application of the resistivity method developed to the Azdavay Carbonife rous area and the correlation of the results obtained with those of well logging surveys.

Several deep resistivity soundings were made in the Azdavay area in order to determine the thicknesses and kinds of the different formations and to correlate them. The locations of these soundings are shown in Fig. 13 (E. S. I, II III. IV, IV, V). For each sounding the electrode separation was expanded from 20 m up to 200-700 m according to the topographical conditions.

For the measurements, the apparatus described in Section I, I.2, with the commutator was used.

Two major kinds of effect played role on the measurements :

1) The effects of the mutual inductance of the current and potential leads and of the self-inductance of the ground included between the potential electrodes.

This kind of effect becomes sensibly large when the electrode separation exceeds 250 m.

2) The effect of the geometrical shape of the ground around the electrodes. The first kinds of effect were eliminated from the measurements as follows :

If the actual resistance and the self-inductance of the ground included between the potential electrodes are R and M, respectively the mutual inductance of the current and potential leads is M, then the effective resistance measured (R') is given by the formula :

$$R' = [R^2 + (L + M)^2 \omega^2]^{1/2}$$

Here ω is the angular velocity of the commutator.

In order to find the actual resistance R, two measurements were made with different commutator speeds at the same electrode separation and the value of R was calculated.

As regards the second kinds of effect, they are treated in detail in Section I. Actually the greatest part of the resistivity measurements were made in the 2-dimensional valleys of the area and the method developed in Section I was applied to them.

I. 21. Analysis of E. S. I.

As seen from Fig. 13, the E. S. I, is located at the junction of the Azdavay-Cide highway and the Değirmendere stream. The curve obtained by the Wenner-Gish - Rooney method is shown in Fig. 14, indicated by the formula

$$\varrho_a = 2\pi a \frac{V}{I}$$

The corrected curve when the corrections for the induction effects are applied is shown in the same figure. It will be seen that when the electrode separation exceeds 300 m the effect is sensibly high. For the electrode separation of 500 m this effect is about 15 % of the actual resistivity value.

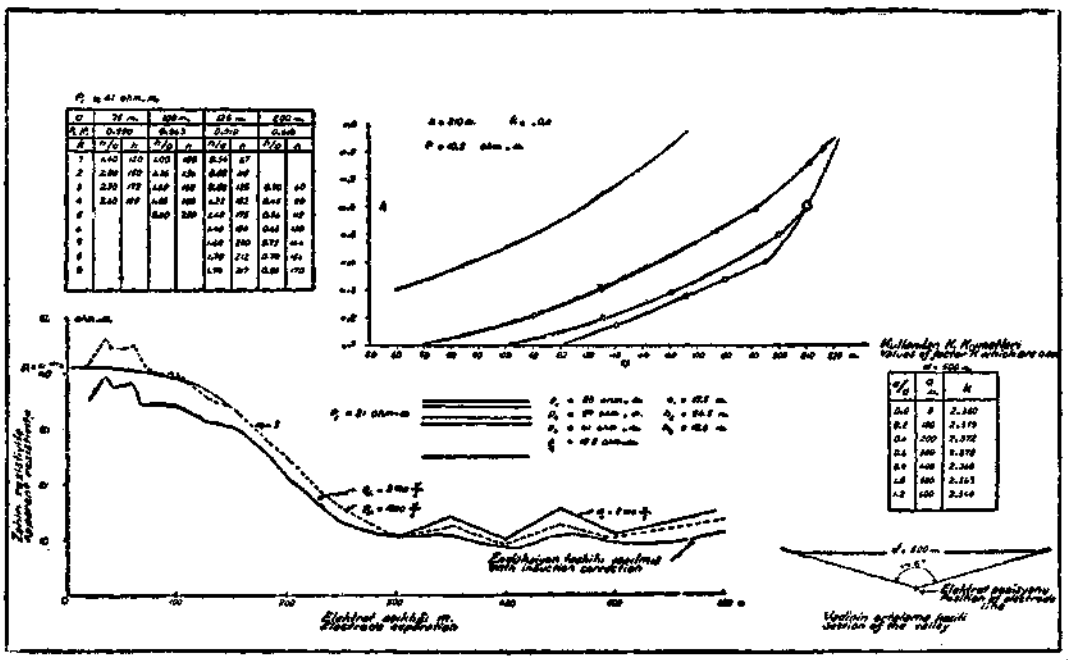

Fig. 14 - Solution of E. S. I

The average section of the valley in which the measurements were taken is shown in Fig. 14. This valley is of triangular section having a width of 500 m and a bottom angle of 146°.

It will be seen that the factor *Ks* for such a valley are determined in Section I (the curve 1' in Fig. 8). The curve obtained using these values is marked I and shown in Fig. 14. The values of this curve are corrected for the induction effects. It is seen from the same figure that the curve $\varrho_a = K\pi a \frac{V}{I}$ cuts the curve $\varrho_a = 2\pi a \frac{V}{I}$ at around $a = 300$ m. On the first part apparent resistivities for the curve $\varrho_a = K\pi a \frac{V}{I}$ are larger than the corresponding ones on the curve $\varrho_a = 2\pi a \frac{V}{I}$. On the last part, the reverse case happens.

The first part of the curve I (a = 0 — 115 m) is drawn on a large scale separately and then solved (see Fig. 15). This curve which exhibits 3 layers is solved using the following principle :

The average resistivity of 2 infinite layers on top of each other having thicknesses h_1 and h_2 and resistivities J_1 and J_2 respectively can be derermined by the formula,

$$\frac{h_1 + h_2}{\varrho \text{ average}} = \frac{h_1}{\varrho_1} + \frac{h_2}{\varrho_2} \quad (1)$$

To solve the curve, the first part of the average curve was extrapolated to cut the axis of the apparent resistivity. This point gave the value of J_1 = 38 ohm-m. A tangent was drawn from this point on the first part of the curve.

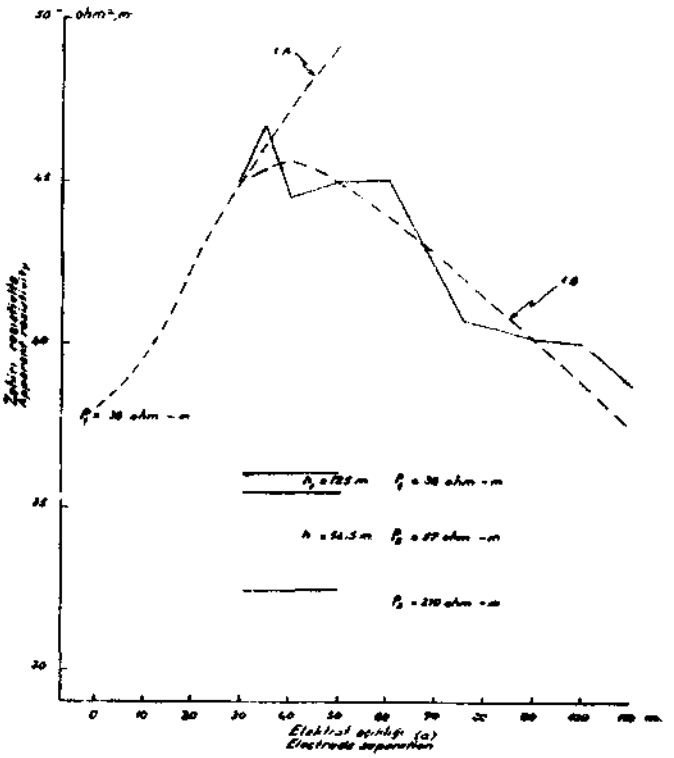

Fig. 15 - Magnified first part of E. S. I

This tangent was solved by the Tagg's method (Fig. 16) and the values h_1= 17.50 m, J_2 = 57 ohm-m were determined. Then the electrode separation corresponding to the inflection point on thes econd part of the curve was determined to be a 110 m. And using the formula h_1 + h_2 = 2/3. a the approximate value

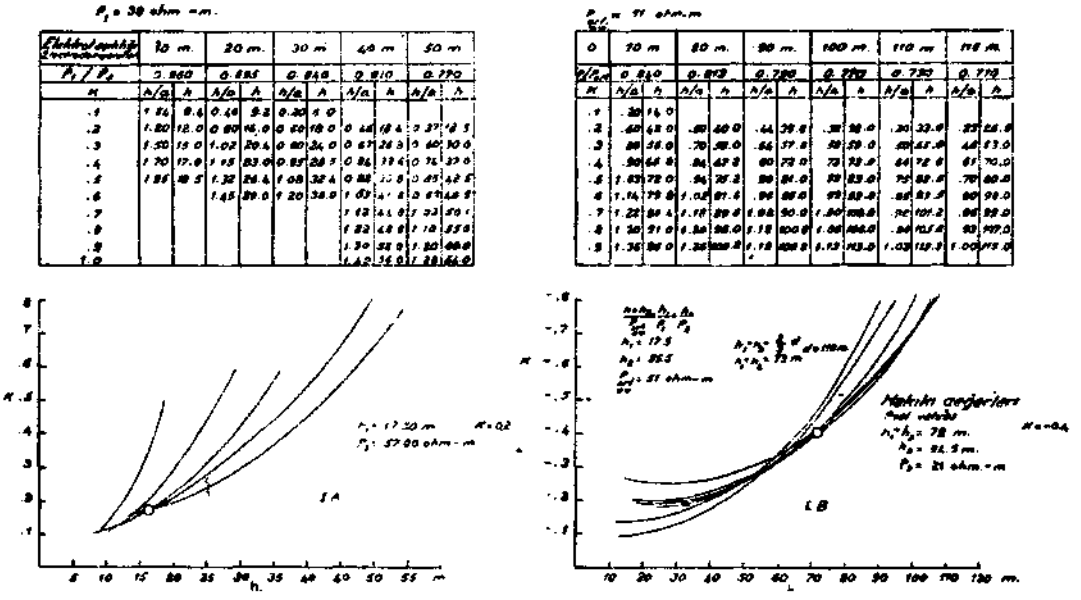

Fig. 16 - Solutions of I A and I B

of h_2 = 55.5 m was found. Replacing the values of J_1, J_2, h_1 and h_2 in formula (1), the value of $J_{av.}$ = 51 ohm-m was determined. And the second part (IB) was solved using this average value by the Tagg's method.

Lastly an average curve was drawn for the whole of the original curve (I), and solved by the same method.

The thicknesses of the formations and their resistivities are shown in Fig. 14. As it will be seen from this figure, the first layer has a low resistivity (38 ohm-m) and a small thickness (17.5 m), this is underlain by a layer with higher resistivity (57 ohm-m) having a larger thickness (54.5m). Below this layer, there is a thin layer with a low resistivity. Then comes a very thick layer (138 m) with a resistivity of (41 ohm-m). This is lastly underlain by a bed having a very low resistivity (10.2 ohm-m).

The comparison and correlation of the results obtained from £. S. I. and those of well logging :

A bore hole (No. 3) was drilled down to 500 m a few meters near the E. S. I. and well logging measurements of resistance and self-potential were taken in the hole, using the single electrode system. The well log obtained and the geological section are shown in Fig. 17.

From the comparison of the well log with the results obtained from E. S. I. it will be seen that the layer 17.5 m thick deduced from E. S. I. corresponds to the alluvium; the underlain layer of 54.5 m thickness again from E. S. I. corresponds to a bed of high resistivity between the depths of 30 and 77.5 m. The definite resistance and self-potential drops at the depth of 225 m on the well logging (Fig. 17), corresponds to the depth of 210 m as deduced from E. S. I.

As a result of the considerations of E. S. I. and the well-log (No. 3), it can be said that there is a permeable and high-resistivity (41 ohm-m) Carboniferous formation extending from the surface down to the depth of 220 m. This layer is underlain by a different Carboniferous layer having a low permeability and resistivity.

I.22. Analysis of E. S. II.

This deep sounding was made on the Permian block as shown in the geological map of Fig. 13, in order to determine its thickness and to see whether the underlain bed is Carboniferous or not. But as seen from the curve obtained in Fig. 18, the apparent resistivities obtained are

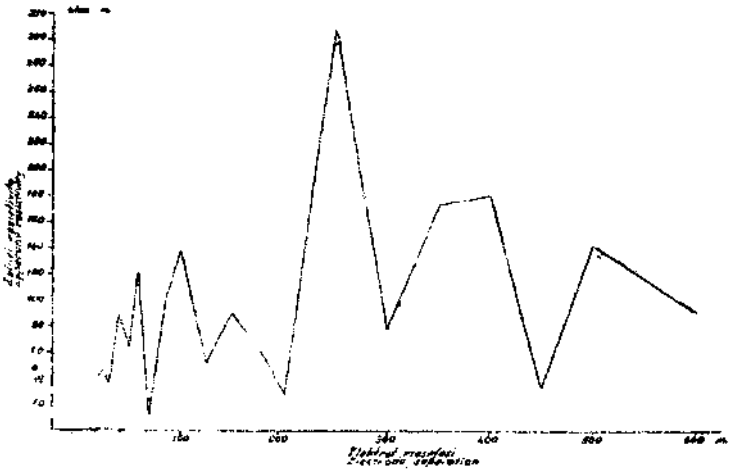

Fig. 18 - Resistivity curve for E. S. II

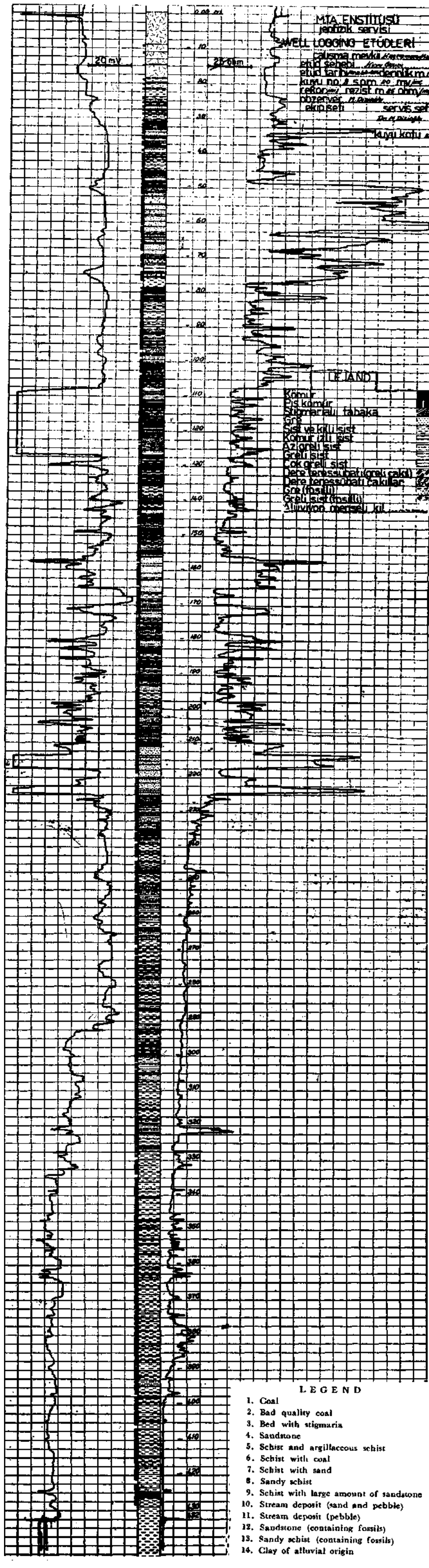
SP.
R.
MTA ENSTİTÜSÜ
jeofizik servisi
WELL LOGGING ETÜDLERİ
çalışma mevkii
etüd sebebi
etüd tarihi
kuyu no
rektor
nezist m
ohm/m
gözlemci
ekip şefi
servis şefi
kuyu kotu
20 mV
25 ohm
LEJAND
Kömür
Kötü kömür
Stigmarialı tabaka
Grè
Şist ve killi şist
Kömür izli şist
Azgreli şist
Grelli şist
Çok grelli şist
Dere teressübatı (grelı çakıl)
Dere teressübatı çakıllar
Şist (fosilli)
Grelı şist (fosilli)
Alüvyon menşeli kil
LEGEND
1. Coal
2. Bad quality coal
3. Bed with stigmaria
4. Sandstone
5. Schist and argillaceous schist
6. Schist with coal
7. Schist with sand
8. Sandy schist
9. Schist with large amount of sandstone
10. Stream deposit (sand and pebble)
11. Stream deposit (pebble)
12. Sandstone (containing fossils)
13. Sandy schist (containing fossils)
14. Clay of alluvial origin

too irregular to be solved by any method. This high variation in the apparent resistivities shows the probability that the area may be faulted and fractured. Actually the seismic survey made over this block later, confirmed this result.

I. 23. Analysis of E. S. III.

To investigate the depth and thickness of the Cretaceous flysch and to learn whether the Carboniferous formation exists below the flysch, this deep sounding was made. The location of this sounding and the curve obtained are shown in Figs. 13 and 19.

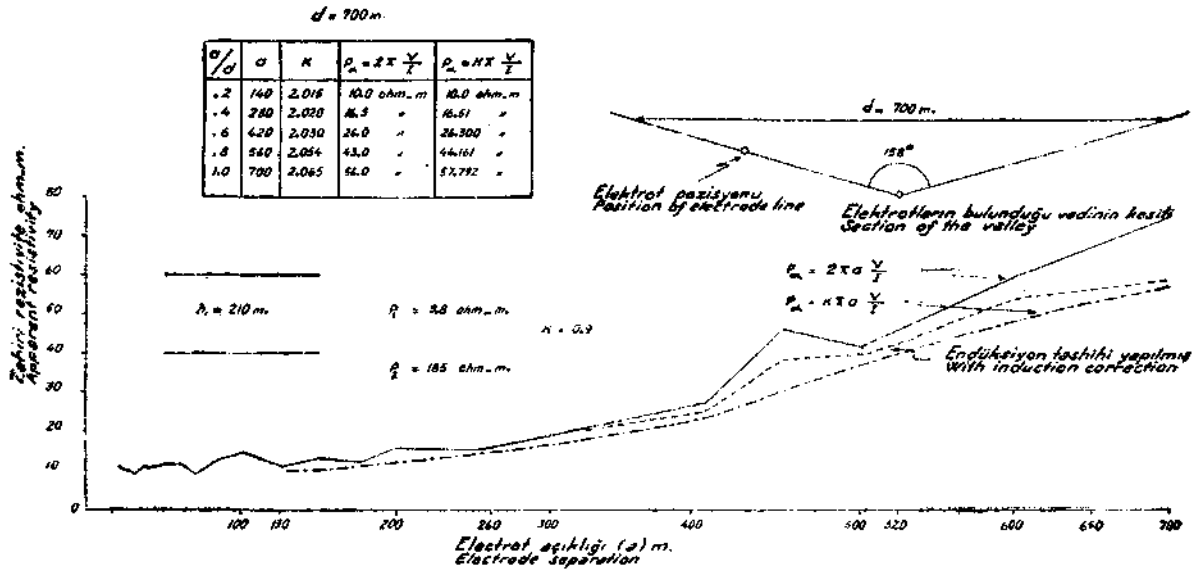

Fig. 19 - Corrections of E. S. III and its Solution

The induction corrections were made for electrode separations greater than 250 m in the same way as for E.S.I. As this sounding was made in a valley of triangular section with a bottom corner angle of 158°, and the electrodes were positioned along the middle of a side, the values of the factor *K* corresponding to this case, which are represented by the curve I' in Fig. 9, Section I, were used in calculating the apparent resistivities, The curve obtained was solved by the logarithmical Tagg's method. The logarithmical curve as shown in Fig. 20 was applied to the logarithmical 2-layer curves and the thickness and the resistivity of the first layer was found to be 210 m and 9.8 ohm-m respectively. This layer is underlain by a bed having a high resistivity (185 ohm-m).

These results indicate that the thickness of the flysch formation at E. S. I. is about 210 m and it is not underlain by. the Carboniferous formation. Judging from the high resistivity this last bed might be limestone.

1.24. Analysis of E. S. IV.

In order to investigate the area around the well No. I, just south of it, 2 deep soundings (IV and IV) were tried at the same point, with the lines of electrodes in different directions. Since with the sounding E.S. IV the electrodes had to be positioned in a thick forest for electrode separations greater than 100 m, this sounding could not be carried out.

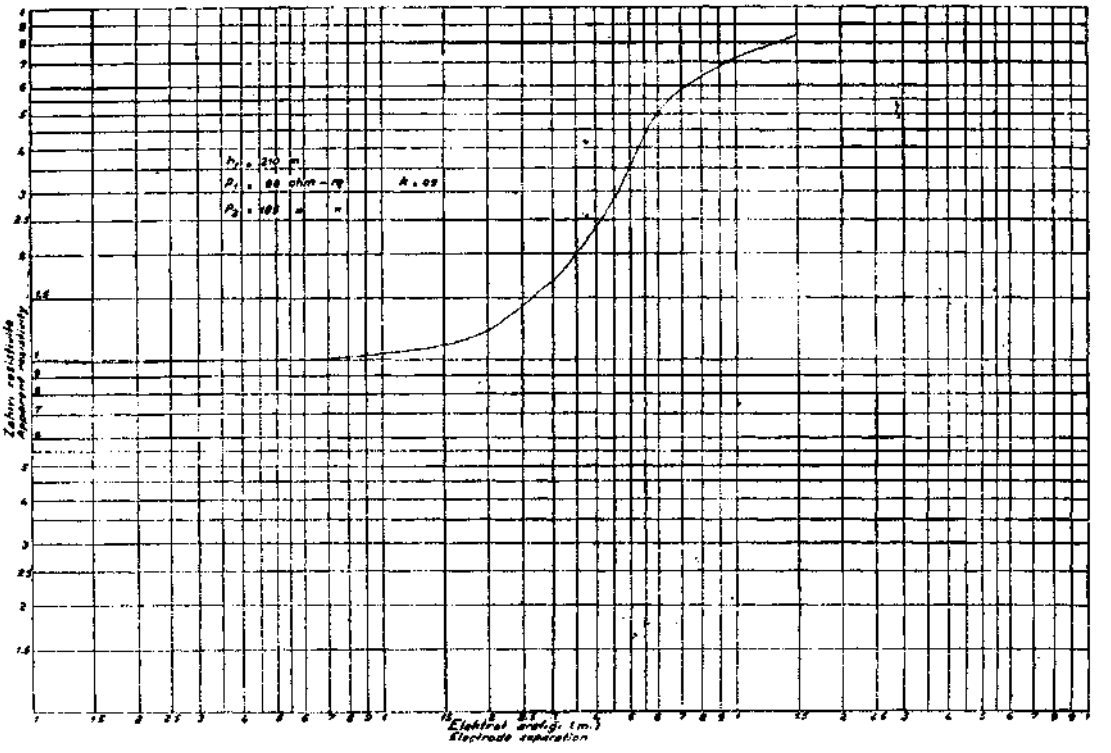

Fig. 20 - Solution of E. S. III by the graphical logarithmic method

The curve for E.S. IV is shown in Fig. 21. The area on which this sounding was made, was fairly flat and the factor *Ks* were taken equal to 2 for all the separations.

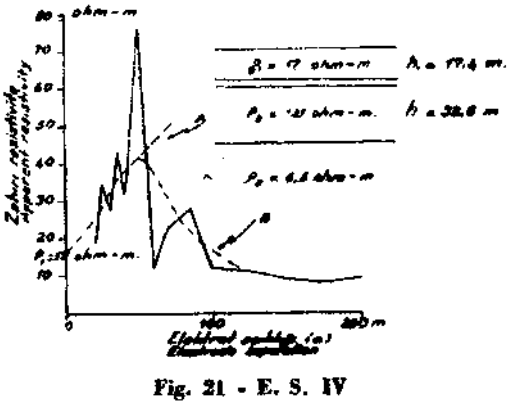

Fig. 21 - E. S. IV

As seen from the average curve for E.S. IV, it exhibits 3 layers. This curve was solved in the same way as for E.S.I, for the 3 layers (see Fig. 22). As a result of this, the thickness and resistivity of the first layer were determined to be 17.4 m and 17 ohm-m. respectively; the middle layer had a thickness of 32.6m and a resistivity of 131.00 ohm-m. At the depth of 50 m below the surface, on the other hand, a formation having very low resistivity (6.6 ohm-m) exists. It is most probable that the first layer may be alluvium, the second one is the sandstone of the Carboniferous age and the 3rd one, an older Carboniferous formation. Because at E.S.I, there was a Carboniferous formation having a resistivity comparable in magnitude with that of this formation. This low resistivity formation started from the depth of 210 m at E.S.I and from the depth of 50 m at E.S.IV. That means that the block on which E.S.IV exists may most probably be 160 m higher stratigraphically than that on which E.S.I is situated.

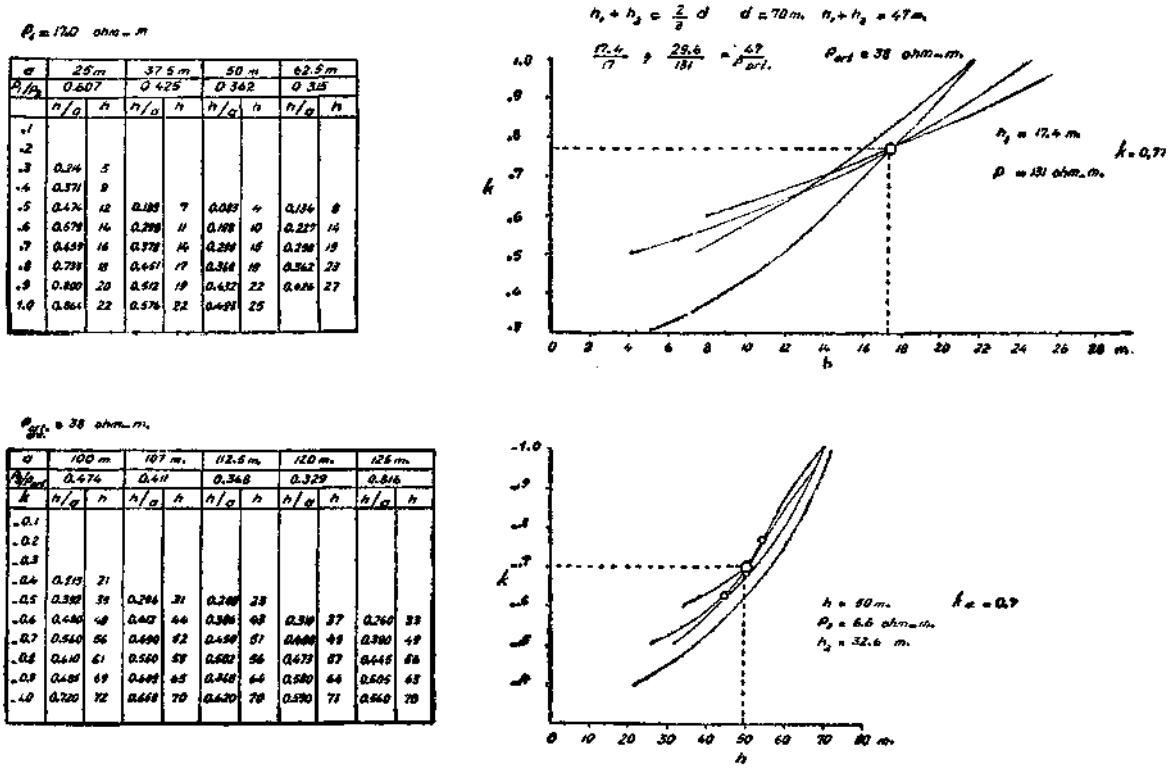

Fig. 22 - Solution of E. S. IV - B

I. 25. Analysis of E. S. V.

This sounding was made in the Devrekani gorge in order to determine the thickness of the Cretaceous limestone outcropping at this locality as well as to investigate whether this limestone is underlain by-the Carboniferous formation.

The average cross-section of the gorge is shown in Fig. 23. The section is almost a right-angle triangle. The values of the factor *K* for such a valley were determined in Section I and the curve 1 in Fig. 8 was obtained. These values were used in the calculation of the apparent resistivities. The correction for the induction effects was made in the same way as in the case of E. S. I.

It will be seen from the curve that the apparent resistivities are quite low for the small separations (smaller than 70 m). This is due to the running water in gorge.

At the electrode separation of 95 m the apparent resistivity rises quite steeply. This may be due to a fault or a dislocation zone near one of the current or potential electrodes.

The part of the curve for the electrode separations larger than 125 m is quite regular and was solved by the graphical logarithmic method.

As a result, the thickness and the resistivity of the first layer were determined to be 80 m and 60 ohm-m. This layer is underlain by a bed having a high resistivity (130 ohm-m).

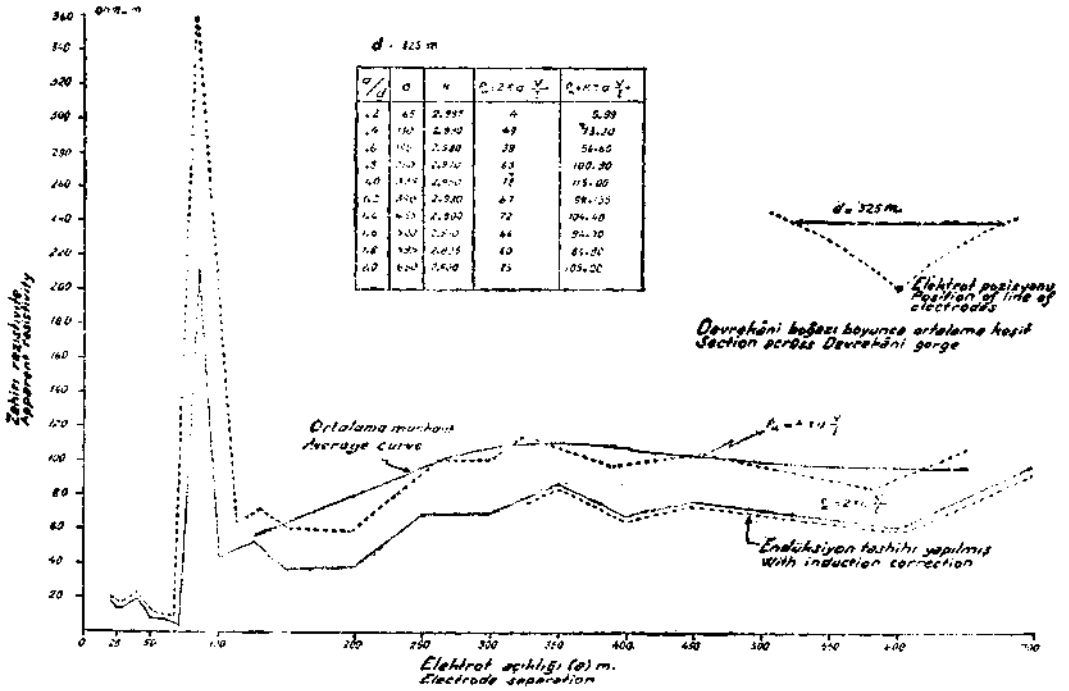

Fig. 23 - Solution of E. S. V

It was deduced from E. S. I. that the average resistivity of the Upper Carboniferous is 41 ohm-m and that of the Lower Carboniferous is about 10 ohm-m. The resistivity values obtained from E. S. V are not of these magnitudes. They are much larger. The 80 m thick layer might be limestone and the underlain high - resistivity bed may probably be the same high-resistivity bed which was determined at the depth of 210 m at E. S. III.

It should be added here that if instead of $\varrho_a = 2\pi a \frac{V}{I}$ the resistivity formula $\varrho_a = K \pi a \frac{V}{I}$ was not applied in determining the apparent resistivities for E. S. V then the resistivity of the first layer would have appeared to be about 40 ohm-m. This result would then lead to conclude that the first layer might be the Upper Carboniferous formation. This conclusion would, however, be quite wrong.

I. 3. Detection and location of fault by the resistivity method in the Azdavay Area.

As seen above from the deep resistivity soundings, there are fairly large resistivity differences between the Carboniferous, Permian and Cretaceous formations in the area. Their resistivities are about 40, 60, 10 ohm-m respectively. These differences were made use of, in detecting and locating the formation contacts as well as the faults.

To this end, several resistivity traverses were run keeping the electrode separation constant. The electrode lines were kept parallel to the supposed formation contact or fault plane. Hence, when the electrodes change formation or are in the fault plane, sudden resistivity changes should occur.

To start with, measurements were taken along the traverse (A, B, C, D, ... N). At each point 2 electrode separations (50 and 100 m) were used. That is to say, 2 constant electrode - separation traverses were run along the same profile. The results obtained are shown in Fig. 24. As seen from the curves, the Permian formation ends at H, east of which Carboniferous formation starts. At K, the electrodes penetrate into the productive Carboniferous (see Fig. 13).

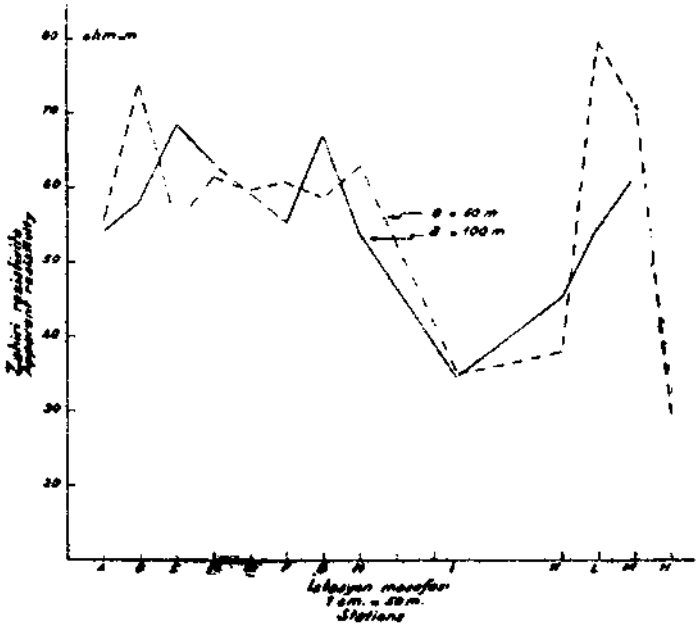

Fig. 24 - Constant separation resistivity traverses (Azdavay Area)

Secondly, the traverse 146-157 was run using different electrode separations (see Fig. 25). The constant separation curves show that the Carboniferous formation is reached at the point 146, and that the apparent resistivities at the point 149 increase sharply. This increase was thought to be due to a fault zone. This idea was later confirmed when the geologists made a detail survey of the area. On the same profile, the average apparent resistivity falls down to 40 ohm-m at the point 150. This indicates that the Carboniferous is again reached at this point.

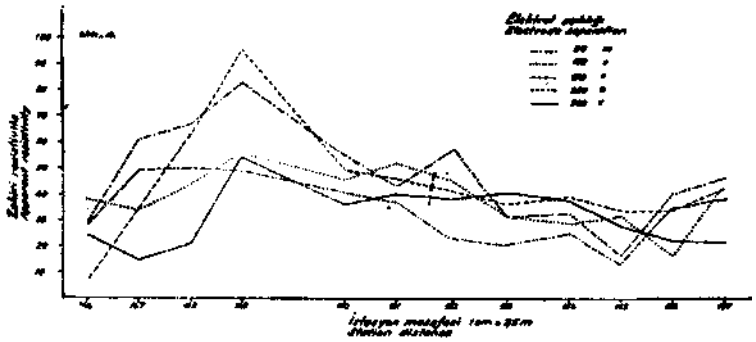

Fig. 25 - Constant separation resistivity traverses (Azdavay Area)

Further south, the curve for the profile I-27 is shown in Fig. 25. It can be judged from the sharp increase of the apparent resistivity at the point 13 that

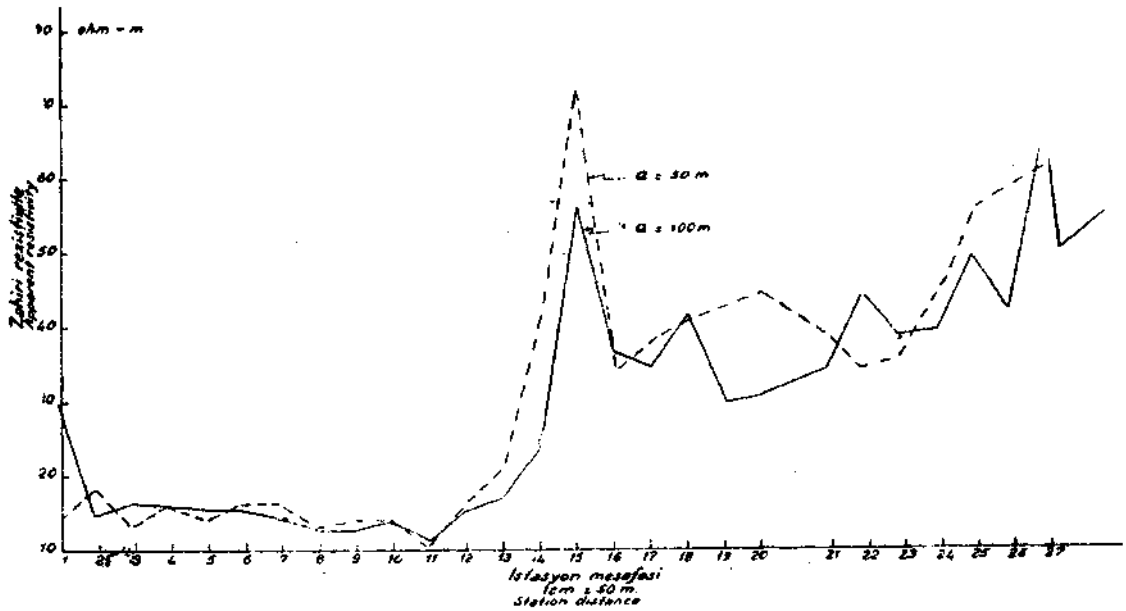

Fig. 26 - Constant separation resistivity traverses (Azdavay Area)

the Cretaceous flysch ends at this point. There is a high jump of resistivity between the Stations 13-16. This corresponds to the fault zone between these stations. The magnitude of the resistivity reaches that of the Carboniferous beyond the Station No. 17. This indicates the existence of the Carboniferous from this station on, as will be seen from Fig. 13. This result is confirmed by the geology.

4 more constant separation traverses were run around hole No. 3 in order to detect and locate the faults, if any, around this hole. These curves are shown in Figs. 27, 28, 29 and 30. The faults inferred from these are shown in the geo-

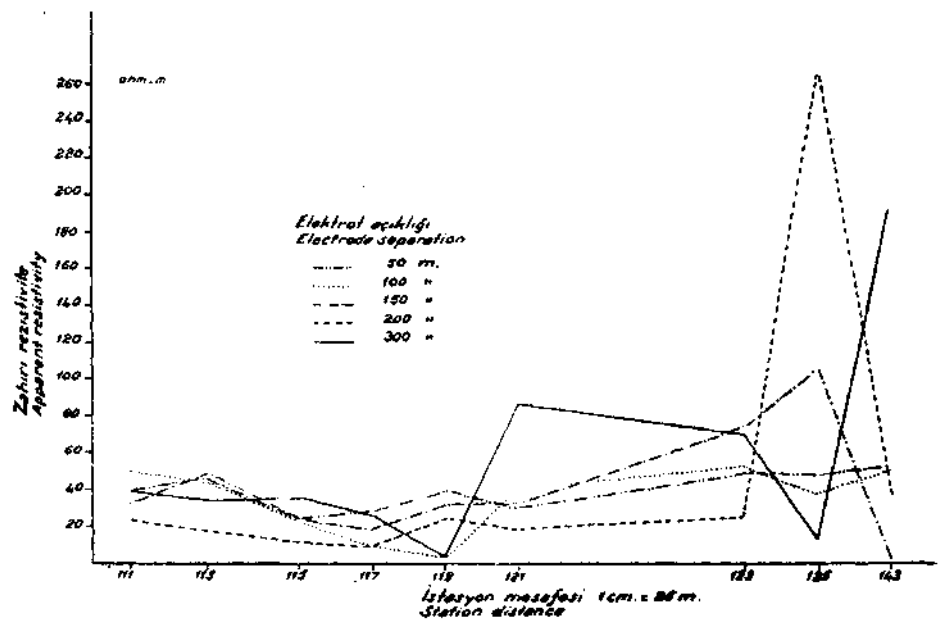

Fig. 27 - Constant separation resistivity traverses (Azdavay Area)

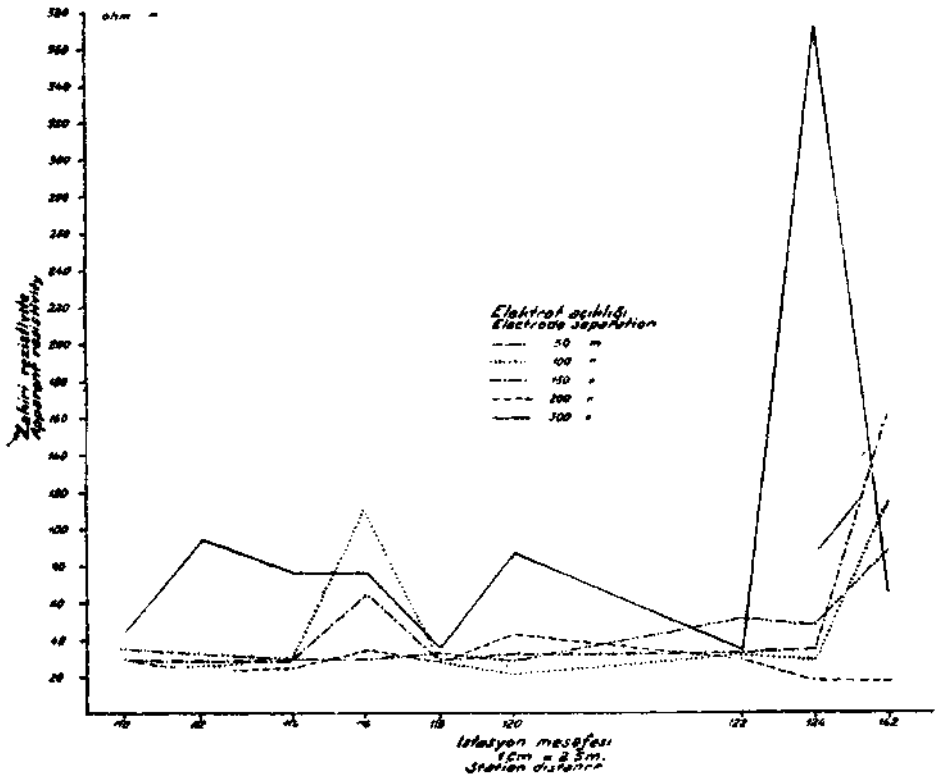

Fig. 28 - Constant separation resistivity traverses (Azdavay Area)

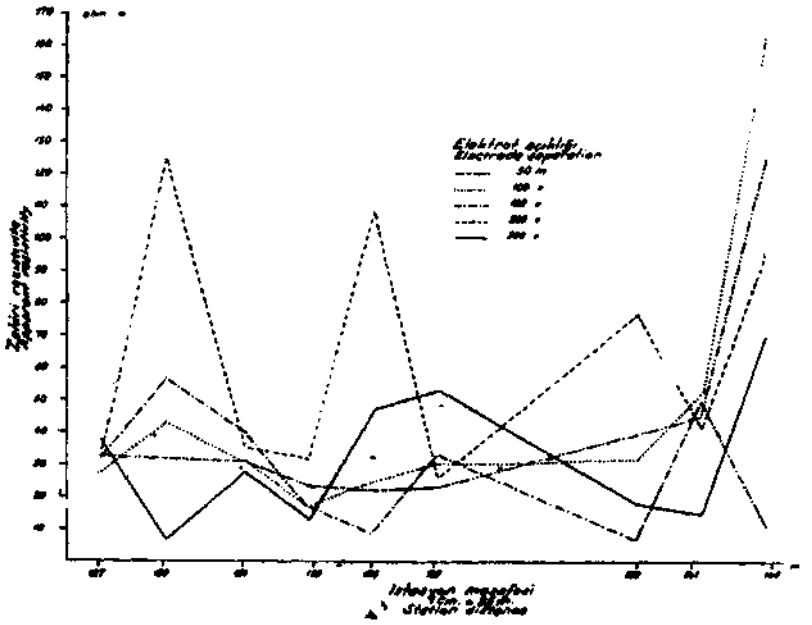

Fig. 29 - Constant separation resistivity traverses (Azdavay Area)

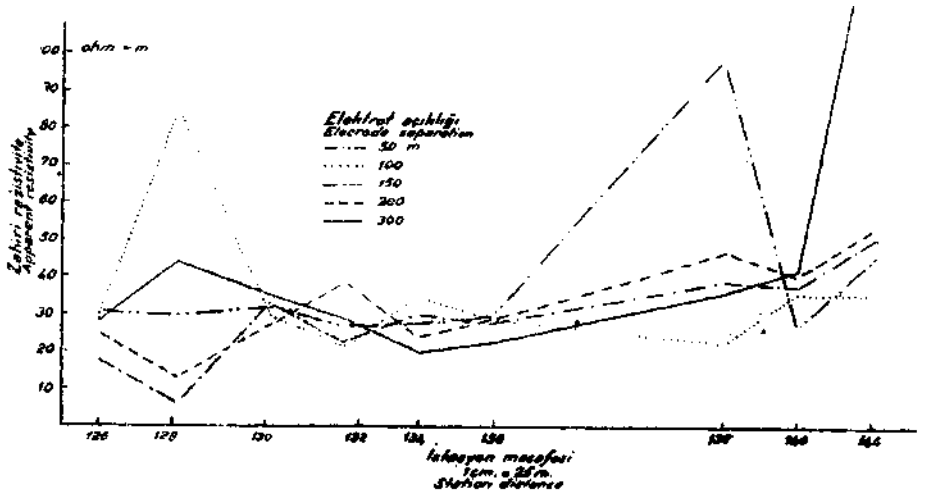

Fig. 30

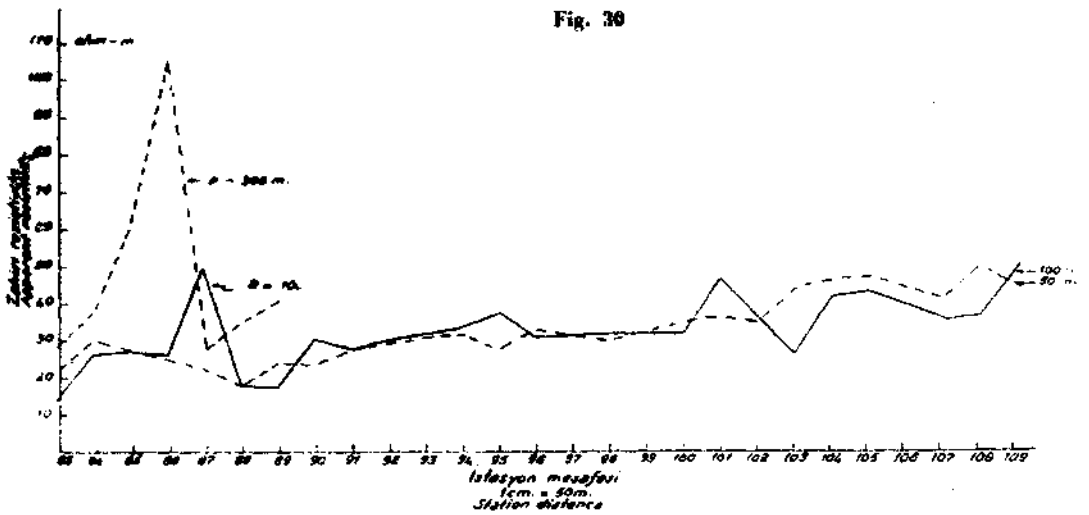

Fig. 31

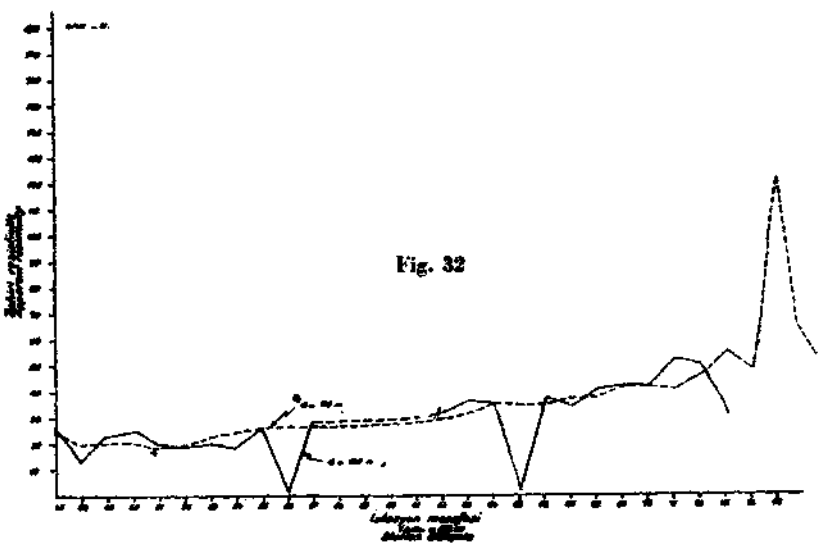

Fig. 32

Figs. 30, 31, 32 - Constant separation resistivity traverses (Azdavay Area)

logical map (Fig. 13). The approximate positions of the faults No. 1 and 2 in the geological map are confirmed, but it was deduced from these curves that they are not so straight as on the map.

Further in the south, the contact between the flysch and Carboniferous formations was investigated. As this area is covered by alluvium, the contact could not be followed by the geological methods. Constant separation traversing was used in these investigations. The curves obtained are shown in Figs. 31, 32, 33 and 34. The locations of the traverses are indicated in Fig. 13 It will be seen from the curves that over the fault zone sharp and high resistivity jumps occur. These jumps are probably due to the crushed and fractured zone of the fault

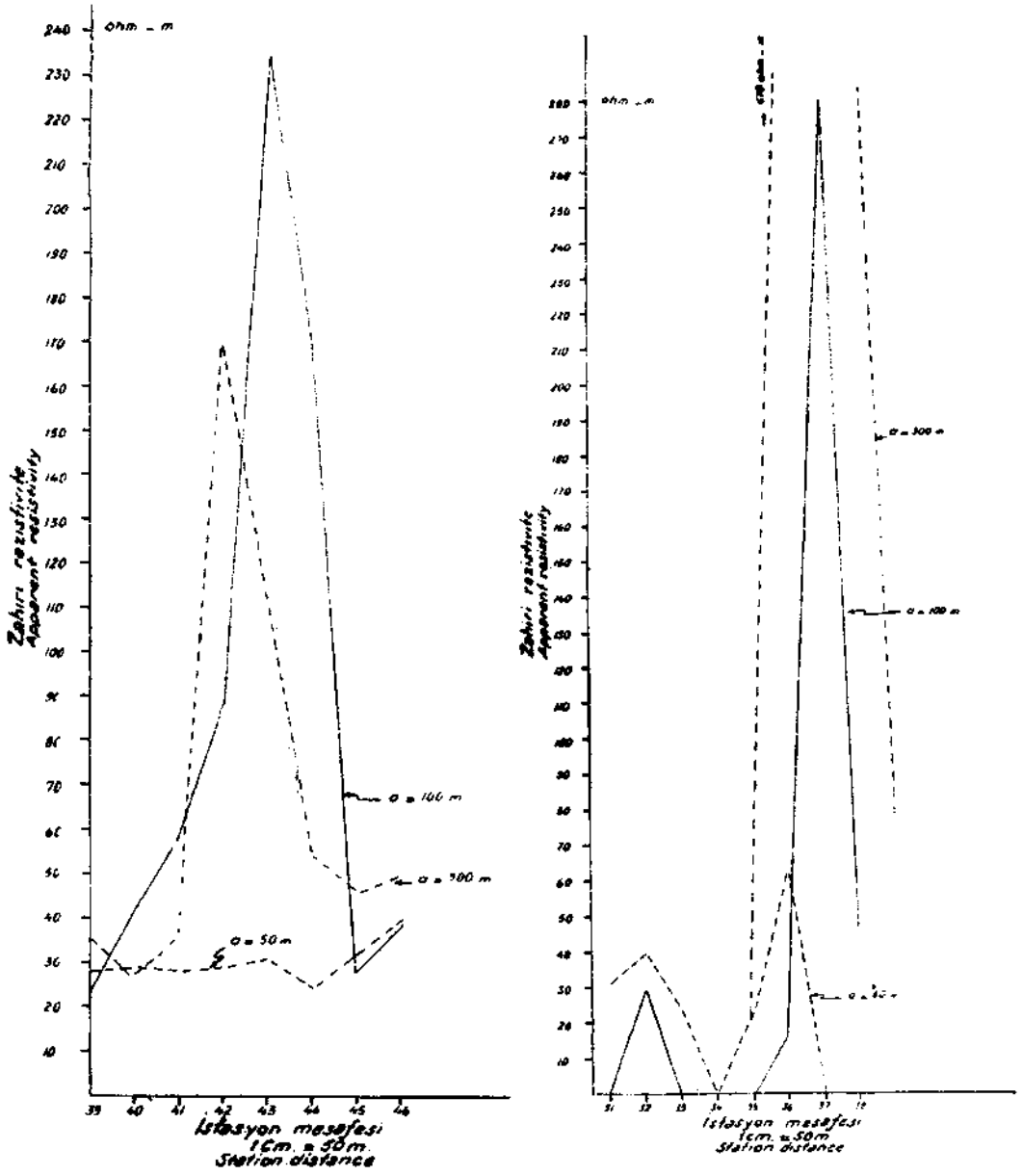

Figs. 33 and 34 - Constant separation resistivity traverses (Azdavay Area)

line. The contact line determined is drawn in Fig. 13. As seen, this contact is not a straigh line, it is curved. This curved line might rather indicate that the contact zone is not that of a fault but that of an overthrust. An important point which could be seen from the Figs. 31, 32, 33 and 34 is that no other signs of fault exist in this block covered by alluvium. Hence the well No. 1 does not enter into this block. Actually, it was deduced from the seismic section along the road forming the northern front of this block that a fault runs along this road. The faults occurring further north do not enter beyond this road into the block. It was concluded from these facts that this block might be a more stable zone and contains the older Carboniferous formation. To verify these results, 3 holes (No. 6, 7, 8) were drilled in this block (see Fig. 13). The formations which were passed through by these holes as well as the electrical well logs taken in these holes by the single electrode system are shown in Figs. 35, 36 and 37. It will be seen from these figures that these holes struck more and thicker coal seams than anywhere else in the region. The total average thickness of the seams in each hole is about 10 m.

The correlation of these holes by means of the resistivity and self-potential logs is shown in Fig. 38. As it will be seen from this figure, the dips down to the depth of 90 m are rather small; but further down the formation changes and the dips become much greater. The contact where the change of dip occurs represents probably a surface of unconformity.

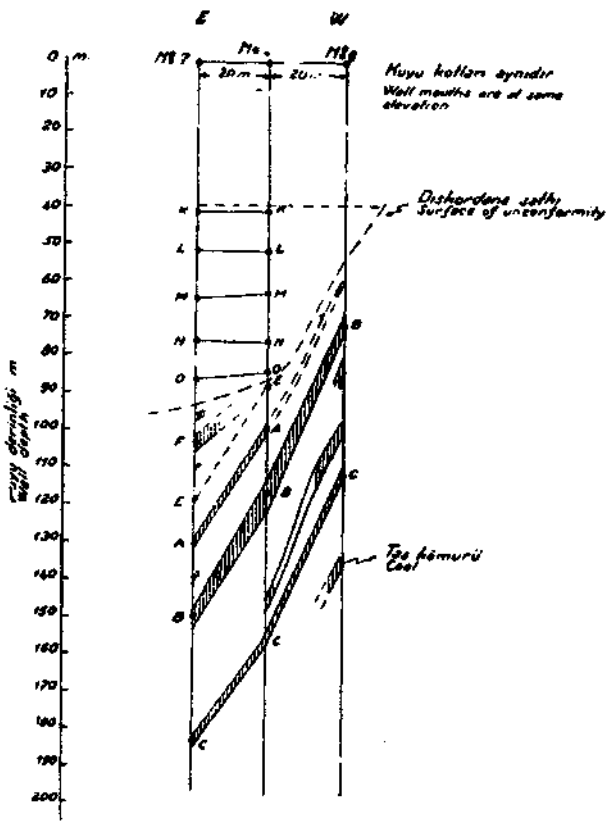

Fig. 38 - Correlation of the well loggings No. 6, 7, 8

I. 4. Correlation of the results obtained from the resistivity survey with those of seismic.

In order to investigate and enlighten the tectonics of the Azdavay area, the reflection seismic profiles shown in Figs. 39 and 40 were made.

I. 41. Method and technique employed in conducting the seismic survey.

In the area surveyed, no reflections with a pulse having characteristic envelopes and elevations could be obtained. The reflection certainties and the reflection dip accuracies are generally fair and bad, and sometimes good. For this reason, the overlapping split set-up type of profiling was used with a view to easing the picking of the reflections on the records and to having a full under-

Well Loggings of Holes (Azdavay - Kastamonu)

Elevation : 815.66 m

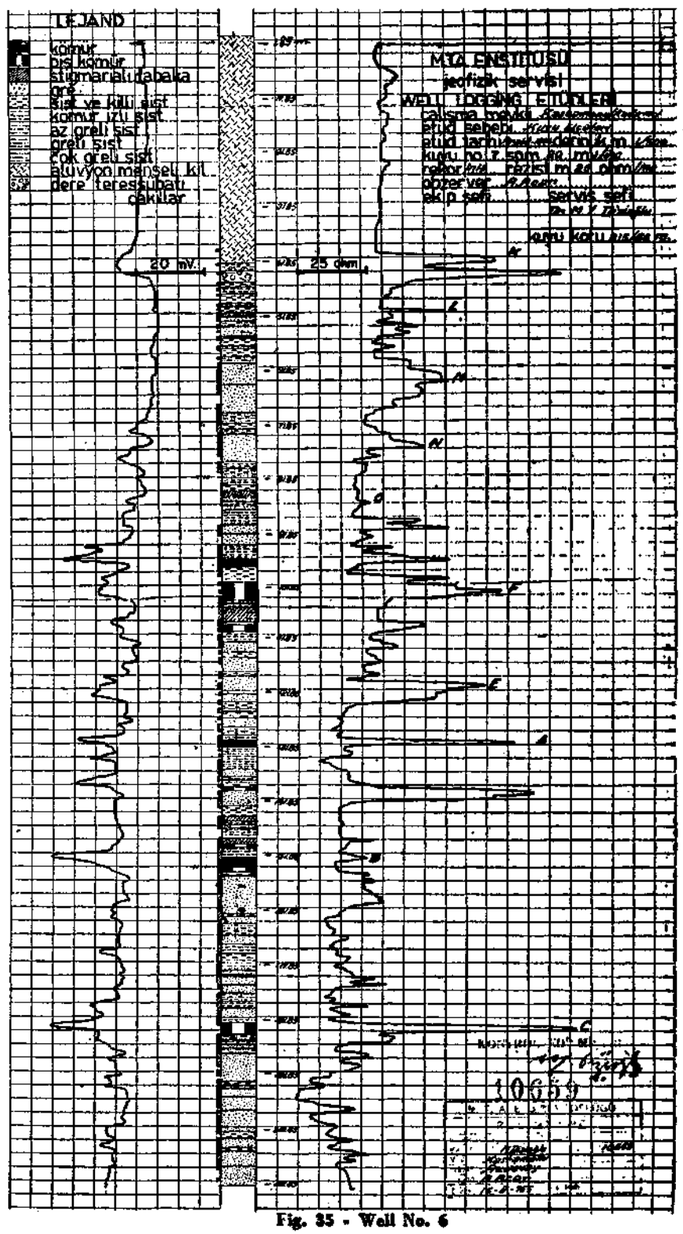

Fig. 35 - Well No. 6

Elevation : 815.73 m

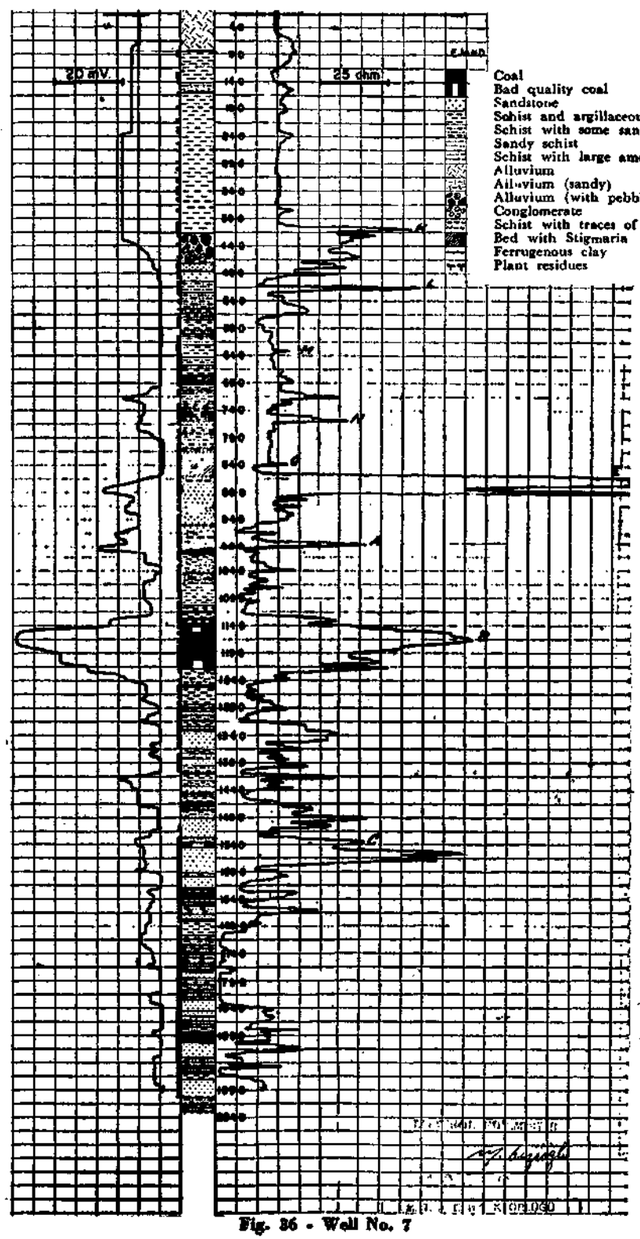

Fig. 36 - Well No. 7

Elevation : 815.75 m

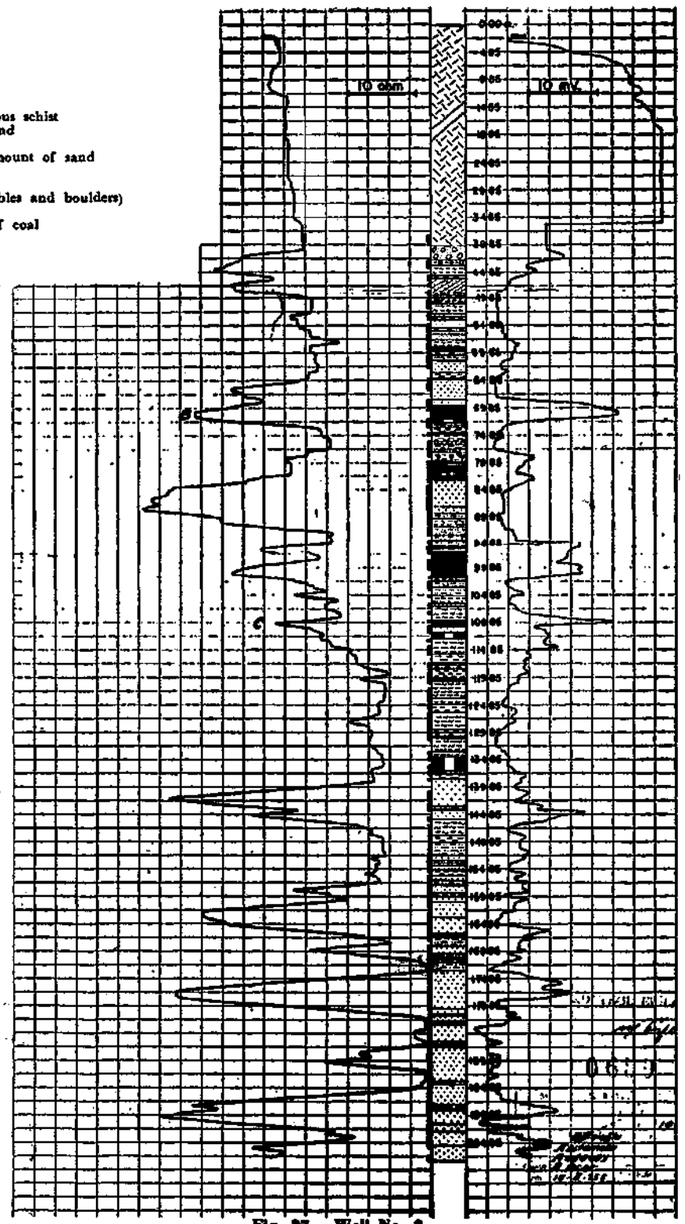

Fig. 37 - Well No. 8

ground control. Whenever possible, it was tried to outlay the profile lines in closed loops.

The best spread was determined to be 210-0-210 m. The shot holes were positioned in the line of the spread, on each side of the spread. And on each side of the shot hole, 11 geophones were positioned at equal intervals.

For recording, the «Reflection Seismograph Recording Unit» (24 trace) mounted on a truck was used. This was manufactured by the Engineering Laboratories Inc.

The best filter setting was determined to be «Selector 2, Frequency 2».

In computing the data obtained, the velocity function of $V_{int.} = V_0 + 0.6\,z$, which was determined by the good reflections on the records, was employed. The datum for the surface corrections was chosen to be 20 m below the surface.

Grading :

The certainties of the reflections were divided into 3 :

Good : Those reflections having the three qualities: envelope, elevation and essential copy.

Fair : Those reflections without distinctive envelope but having the remaining qualities.

Poor : Those reflections having only essential copy.

The dip accuracies of the reflections were divided into 3 :

Good : Those having unique alignment and duplicating alignment.

Fair : Those having unique alignment but variable duplication.

Poor : Unique alignment but no duplication.

In this survey, the certainties and the dip accuracies of the reflections were about the same.

I. 42. Results obtained; their interpretation and their correlation with those of resistivity survey.

The two seismic profiles obtained are shown in Figs. 39 and 40 The locations of the shot holes are indicated on the geological map in Fig. 13.

The different blocks and formations as seen in these sections are determined by studying the variation of the velocity of the reflections with depth. Each block had a characteristic average longitudinal velocity.

From the seismic profile along the highway Azdavay-Cide (1-70) these results could be obtained:

1) The dips are relatively regular at depths beyond 400-800 m, between the shot holes No. 8 and 64. This fact indicates that the stable Carboniferous formation exists most probably at deeper levels. The dips above this stable zone are quite irregular.

2) Different blocks are pushed into the Upper Carboniferous which lies above the more stable zone. The parts Lying between different blocks are faulty. These blocks and the formations are determined, as mentioned above, by velocity variation of the reflection with depth.

3) There is a great fault zone lyihg between the shot holes No. 7 and 10. This was inferred to by the lack of reflection and the existence of «drop» and «increased dip» type of reflections below the fault planes.

It is most probable that the block lying southeast of these shot holes is collapsed down.

This fault zone happens to be located around the deep hole No. 1. Actually, at the same area different faults were detected and located by the resistivity survey treated above (Fig. 13). Hence, the results of the two surveys check each other.

A reflection seismic survey was run across the block on which the holes No. 6, 7, 8 are situated. And the seismic holes No. 105, 104, 103, and 102 were shot. The results of these shots are shown in Fig. 40. As will be seen, this block consists of a syncline. The holes No. 6, 7, 8 are located between the shot holes No. 104 and 103. The dips obtained check those found by the well logging.

SUMMARY OF SECTION I AND II AND GENERAL CONCLUSIONS

First, the need of the development of a resistivity method of prospecting applicable in 2-dimensional valleys was pointed out and different ways of development were discussed. Among these ways, that by the small-scale model experiments was preferred. The reasons for this preference were, in turn, explained.

By means of the model experiments, the values of the factor K were determined for different types of valley, with different positions of the electrodes. And its variation with the type of valley and the position of electrodes was studied.

Then the directional resolving power of the method developed was investigated.

The method so developed was then applied in the Azdavay Carboniferous area, with a view to determining the depths, thicknesses and types of various formations. The results obtained were compared and correlated with the known geology as well as with the results of the seismic and well logging surveys conducted in the same area.

The general conclusions obtained are as follows :

1) In choosing the appropriate value of the factor K, it is necessary to know the type of the valley and the position of the line of electrodes.

2) The rate of change of the factor K with the ratio a/d (where a= electrode spacing; d= width of the valley) is very large for the values of a/d from 0 to 5. Hence, it is to be careful in choosing the values of the factor in this interval. In the interpretation of the resistivity curves, the part of the curve belonging to this interval should also be regarded with care.

3) The rate of variation of the factor K with a/d, for the values of a/d beyond 8 is rather small and the effect of the valley is quite small. Accordingly, the values of the factor in this interval could be chosen quite accurately. And in the interpretation the error coming from this source could be neglected.

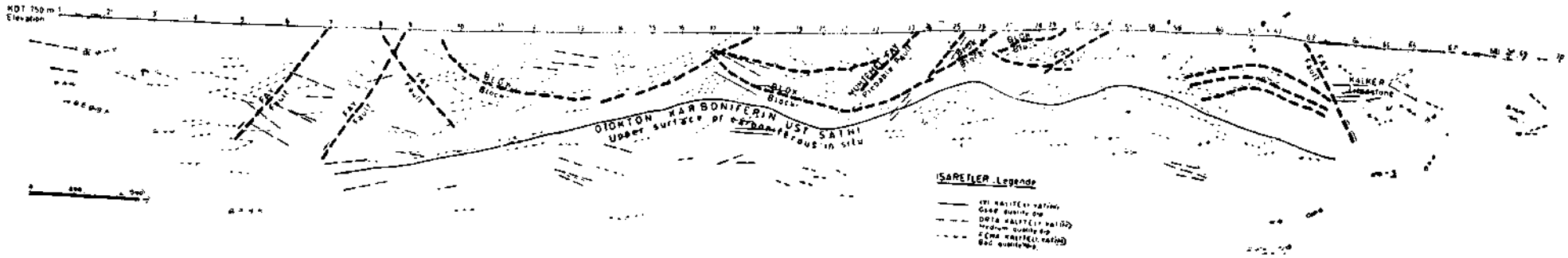

Fig. 39 - Reflection seismic profile along the highway Azdavay - Cide (Party Chief : M. Dizioğlu)

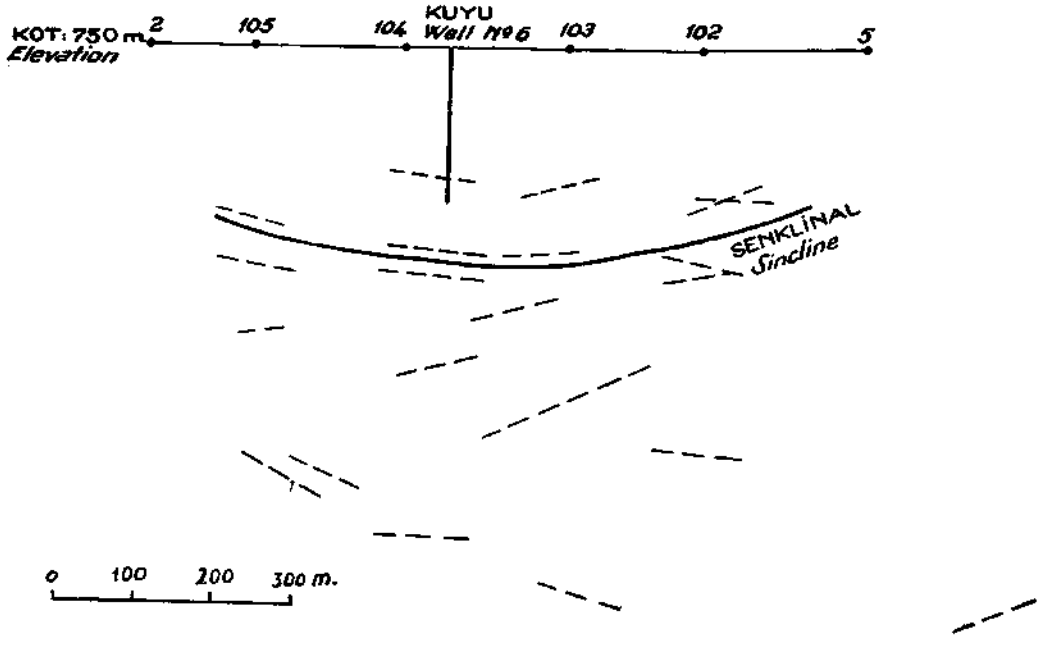

Fig. 40 - Reflection seismic profile along the Topalak Çayı. Scale 1 : 5000
(Party Chief : M. Dinioğlu)

4) If the body producing the anomaly is near the valley, then the small electrode separations are more effective than the large ones in delineating the direction of the body.

5) The method developed must be employed, if the type of the formation, the true resistivity of the formation, and the correlation of different beds are desired.

ACKNOWLEDGMENTS. — The surveys of the Azdavay Carboniferous area, by different geophysical methods, used in this thesis were conducted by the field parties headed by me, for the M.T.A. Institute.

I would like to thank our General Director Ord. Prof. Hamit Nafiz Pamir, (1955), for letting me use these surveys and for his encouraging advice.

I would also like to extend my thanks to observer-computers Muhittin Özyazıcı and Sırrı Kavlakoğlu for correcting the typing errors of the manuscript as well as for helping arrange the figures in the text.

Manustript received July 7, 1959

REFERENCES

1 — WENNER, F. (1916) : A method of measuring earth resistivity. *Bull. U. S. Burcau of Standards,* vol. 12.

2 — HUMMEL, J. N. (1929) : Der scheinbare spezifische Wiederstand. *Zeitschr. für Geophysik,* vol. 5, p. 89.

3 — ZIJLSTRA, G. (1952) : Report on the Azdavay Carboniferous Inlier. *M. T. A. Arch. Rep.* No. 2033.

BIBLIOGRAPHY

1 — SCHLUMBERGER, *I.* C. and M. & LEONARDON, E. G. (1934) : Some observations concerning electrical measurements in anisotropic media and their interpretations. *A. I. M. E. Geophysical Prospecting,* pp. 159-181.

2 — HUMMEL, F. H. *(1929) :* Investigations of potential distribution around various bodies occurring in a homogeneous current field. *Gerlands Beitrage zur Geophysik,* vol. 21, pp. 204-214.

3 — ALDREDGE, R. F. (1937) : *Colo. Sch. Mines Quart.,* 32 (I), Jan. 1937, pp. 171-186.

4 — HEILAND, C. A. (1946) : Geophysical exploration. lst ed. *Prentice Halt, Inc.,* New York.

5 - JAKOVSKY, J. J. (1950) : Exploration Geophysics. 2nd ed., Los Angeles.

6 — HUMMEL, J. N. (1932) : A theoretical study of apparent resistivity in surface potential methods. *A. I. M. E. Geophysical Prospecting,* p. 392.

7 — SMARTZ, T. H. (1931) : Resistivity measurements upon artifical beds. *U. S. Bureau of Mines,* Information Circular 6145, Feb. 1931.

8 — MAILLET, R. & DOLL, H. G. (1932) : Sur un theorerne, relatif aux milieux electriquement anisotropes et ses applications a la prospection electrique en courant continu. *Ergenzungshefte für angewandte Geophysik,* vol. 3, No. 1.